

Journal Pre-proof

Co-combustion of residual forest biomass and sludge in a pilot-scale bubbling fluidized bed

D.T. Pio, L.A.C. Tarelho, T.F.V. Nunes, M.F. Baptista, M.A.A. Matos



PII: S0959-6526(19)34179-4

DOI: <https://doi.org/10.1016/j.jclepro.2019.119309>

Reference: JCLP 119309

To appear in: *Journal of Cleaner Production*

Received Date: 11 July 2019

Revised Date: 11 November 2019

Accepted Date: 12 November 2019

Please cite this article as: Pio DT, Tarelho LAC, Nunes TFV, Baptista MF, Matos MAA, Co-combustion of residual forest biomass and sludge in a pilot-scale bubbling fluidized bed, *Journal of Cleaner Production* (2019), doi: <https://doi.org/10.1016/j.jclepro.2019.119309>.

This is a PDF file of an article that has undergone enhancements after acceptance, such as the addition of a cover page and metadata, and formatting for readability, but it is not yet the definitive version of record. This version will undergo additional copyediting, typesetting and review before it is published in its final form, but we are providing this version to give early visibility of the article. Please note that, during the production process, errors may be discovered which could affect the content, and all legal disclaimers that apply to the journal pertain.

© 2019 Published by Elsevier Ltd.

Daniel Torrão Pio (D.T. Pio): Methodology, Investigation, Formal analysis, Writing – Original Draft, Writing – Review & Editing, Visualization

Luís António da Cruz Tarelho (L.A.C. Tarelho): Conceptualization, Methodology, Investigation, Writing – Review & Editing, Supervision, Project administration

Teresa Filomena Viera Nunes (T.F.V. Nunes): Methodology, Investigation

Miguel Filipe Baptista (M.F. Baptista): Investigation

Manuel Arlindo Amador de Matos (M.A.A. Matos): Methodology, Investigation

Journal Pre-proof

1 **Co-combustion of residual forest biomass and sludge in a pilot-scale bubbling**
2 **fluidized bed**

3 D.T. Pio*, L.A.C. Tarelho, T.F.V. Nunes, M.F. Baptista, M.A.A. Matos

4 Department of Environment and Planning & Centre for Environmental and Marine
5 Studies (CESAM)

6 University of Aveiro, Campus Universitário de Santiago, 3810-193 Aveiro, Portugal

7 *Corresponding author: danieltp@ua.pt (D.T. Pio)

8 **Abstract**

9 Keywords: biomass, sludge, bubbling fluidized bed, combustion, chlorine

10 **Abstract**

11 In this work, the co-combustion of residual forest biomass from eucalyptus and its
12 blend with different amounts of primary and secondary sludge from the pulp and paper
13 industry was studied in a pilot-scale bubbling fluidized bed reactor. The main objective
14 was the determination of sludge addition influence on the overall process and on the
15 composition of the exhaust gases, with emphasis on chlorine emissions, namely
16 present in the solid phase (fly ashes) and in the gaseous phase (hydrogen chloride),
17 and nitrogen oxides emissions. The co-combustion process of residual forest biomass
18 with primary sludge (up to 5% in mass) and secondary sludge (up to 10% in mass) was
19 successfully demonstrated as a valid energy valorization option. Except specific cases,
20 no significant emissions increase of nitrogen oxides, carbon monoxide or hydrogen
21 chloride were found with the addition of sludge. In fact, hydrogen chloride emissions
22 decreased, potentially due to an increase in the chlorine retention in ashes caused by
23 the high inorganic content present in the sludge. This high inorganic content can also
24 lead to a significant increase in ash production during the combustion process. Thus,
25 consequently, without proper maintenance, significant ash accumulation along the
26 combustion system may occur, which can decrease the process efficiency and cause
27 equipment damage.

28

29 **Word count:** 7511 (excluding references)

30 **Abbreviations**

31	BAT	Best Available Technologies
32	BFB	Bubbling Fluidized Bed
33	EL	Experiments with secondary sludge
34	ELP	Experiments with primary sludge
35	ELV	Emission Limit Value
36	FTIR	Fourier Transform Infrared Spectroscopy
37	HTSU	High Temperature Sampling Unit
38	ICP-MS	Inductively Coupled Plasma Mass Spectrometry
39	RFB	Residual Forest Biomass

40

41

Journal Pre-proof

42 1. Introduction

43 Sewage sludge is an unavoidable byproduct of wastewater treatment processes
44 (Hao et al., 2018). This byproduct has been accumulating in the recent years due to
45 lack of proper valorization and disposal methods (Sung et al., 2018). In countries that
46 produce pulp and paper, primary and secondary sludges from the pulp and paper
47 industry may account for more sludge production than municipal wastewater treatment
48 plants (Meyer et al., 2018). Co-combustion of these wastes with other fuels (e.g.,
49 residual forest biomass) is recognized as possible, due to the relatively moderate
50 calorific value of sludges (Kijo-Kleczkowska et al., 2016; Zhao et al., 2019). This
51 process is also promising because it allows the reduction of the sludge volume to be
52 disposed, as well as its energetic valorization by production of heat and power (Chen et
53 al., 2019). Furthermore, both waste sludge and residual forest biomass (RFB) from
54 eucalyptus are byproducts from the pulp and paper industry and considered as
55 potential alternative fuels and renewable energy resources (Sung et al., 2018).
56 Regarding solid and exhaust gases emissions, it is commonly suggested that adding
57 sludges to the combustion process of Cl-rich fuels may reduce chlorine (Cl) deposition
58 and bed agglomeration, while increasing NO_x emissions, due to the sludges high
59 nitrogen content, and Cl gaseous emissions (HCl) (Aho et al., 2010; Aho and
60 Silvennoinen, 2004; Åmand et al., 2006; Åmand and Leckner, 2004).

61 Cl emissions are associated with diverse problems of deposition and corrosion in
62 combustion systems. During biomass combustion processes, the Cl present in the fuel
63 is released and can be present in both gas phase and solid phase. Furthermore, Cl can
64 ease the mobilization of diverse inorganic compounds (Strömberg and Björkman,
65 1997), such as alkali metals present in the burning biomass particles, easing the
66 reaction between these and other substances (Xie and Ma, 2014). Thus, Cl contributes
67 to the increase of problems related to the alkali metals, such as corrosion and
68 agglomeration in the combustion system. Depending on the temperature, it is
69 recognized that a high Cl content in the fuel can cause a significant increase of the

70 emissions of alkali metals (Olsson et al., 1997). Nonetheless, Cl release from the
71 combustion particles can be controlled to a certain point by limiting the maximum
72 temperature of the process (Jensen et al., 2000). Thus, the higher Cl content present in
73 biomass (in comparison with coal (Lokare S.S., 2008)), limit the steam production
74 process conditions in biomass combustion systems, due to temperature limitations
75 (Hupa, 2012; Nielsen et al., 2000; Viklund, 2013).

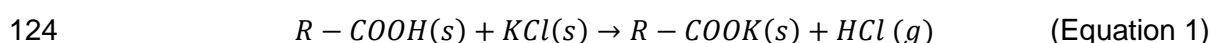
76 Cl release during the devolatilization phase is related to the organic and inorganic
77 fractions of Cl present in the fuel. Cl released at low temperature is associated to
78 organic compounds or HCl and can be recaptured in the chars by secondary reactions
79 with available alkali metals (Johansen et al., 2011). Then, re-release of the captured Cl
80 can occur due to KCl sublimation during pyrolysis and combustion at high temperatures
81 (Johansen et al., 2011). Thus, all relevant Cl species involved in combustion processes
82 are highly volatile, and a high volatilization of Cl is expected (Johansen et al., 2011;
83 Loo and Koppejan, 2008).

84 Accordingly, Lith et al., (Lith et al., 2004) observed high Cl percentage release,
85 including complete dechlorination, during combustion of spruce and fiberboard with
86 process temperature between 500 and 850°C. Diaz-Ramírez et al., (Díaz-Ramírez et
87 al., 2014) observed Cl release near 50% at temperatures below 700°C and complete
88 dechlorination at around 800°C, during brassica and poplar combustion. Strömberg
89 and Björkman (1997) studied the pyrolysis and gasification of different types of
90 biomass (sugarcane trash, switch grass, lucerne and straw rape) and observed that
91 under biomass pyrolysis and gasification conditions, Cl release under 200°C is not
92 significant, 20-50% of Cl was released at low temperatures such as 300 to 400°C, and
93 30-60% of the total Cl was still left in the chars at 900°C. Jensen et al., (Jensen et al.,
94 2000) studied the release and transformation of K and Cl as a function of temperature
95 during the pyrolysis of straw in a laboratory batch operated reactor. The authors
96 observed the release of Cl in two main phases: 60% was released when the
97 temperature was raised from 200°C to 400°C and the remaining fraction was released

98 at temperatures between 700 and 900°C. Knudsen et al. (Knudsen et al., 2004),
99 observed that 25 to 75% of the Cl present in the fuel was released to the gaseous
100 phase at temperatures lower than 500°C, during combustion experiments with different
101 types of biomass. Afterwards, the Cl was released by volatilization under KCl form,
102 mostly between 700 and 800°C. For temperatures above 800°C, the authors observed
103 complete dechlorination for all experiments performed.

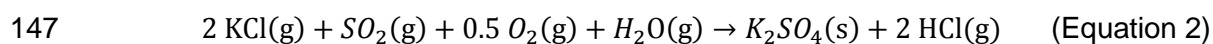
104 During devolatilization (200-400°C), Cl is released to the gaseous phase mainly
105 under HCl form (van Lith et al., 2006); at these relatively low temperatures, the free Cl
106 ion tends to react with hydrogen ions to form HCl, but not with alkaline metals to form
107 alkali chlorines. With temperature increase, HCl formation tends to decrease (Xie and
108 Ma, 2014). For higher temperatures, a significant part of Cl is released under KCl form
109 and associated to char combustion (Díaz-Ramírez et al., 2014; Jensen et al., 2000;
110 Knudsen et al., 2004; Xie and Ma, 2014). After formation and release to the gaseous
111 phase in the combustion system, the alkali chlorines tend to condensate over fly ash
112 particles or heat exchangers (Loo and Koppejan, 2008). Thus, part of the released Cl
113 during biomass combustion seems to become associated to the solid phase of the
114 exhaust gases, namely fly ashes, or deposited in heat exchangers, while the other part
115 is emitted in the gaseous phase as HCl in the exhaust gas (Loo and Koppejan, 2008).

116 Due to the close relation between K and Cl, the release behavior and reaction
117 mechanism of these species is dependent on their initial molar ratio present in the
118 biomass (Johansen et al., 2011). The major Cl compound in biomass is KCl, which is
119 stable in solid phase until temperatures of 700°C to 800°C are attained (Johansen et
120 al., 2011); for temperatures lower than 700°C to 800°C, the vapor pressure of KCl is
121 negligible (Johansen et al., 2011). Nonetheless, the Cl initially present as KCl can react
122 with functional groups present in the organic matrix of the biomass, leading to release
123 of HCl according to equation 1 (van Lith et al., 2006):



125 Jensen et al., (Jensen et al., 2000) suggested that at temperatures between 200
126 and 400°C, the original organic matrix of the biomass is destroyed, and Cl can be
127 released from the solid phase and transferred to a liquid tar phase. Afterwards, Cl is
128 further released to the gaseous phase in the form of HCl (g) or suffers secondary
129 reactions with K on the char surface. Some further release of Cl under the form of HCl
130 might be due to the reaction of KCl with functional oxygenated groups present in the
131 chars, where HCl is released and K is bound to the char matrix. Jensen et al., (Jensen
132 et al., 2000) concluded that by using adequate operating conditions, for example, low
133 heating rates and large reactors, HCl emissions in gaseous phase can be significantly
134 minimized during biomass pyrolysis.

135 As previously referred, the biomass type has a considerable influence on the Cl
136 emissions (Díaz-Ramírez et al., 2014; Knudsen et al., 2004). Some studies suggest
137 that the percentages of Cl emitted, in relation to the Cl content present in the fuel, are
138 significantly higher for fuels with less Cl content, due to the fact that Cl emissions are
139 conditioned by the number of proton donors, such as carboxyl and phenolic groups
140 (Díaz-Ramírez et al., 2014; Knudsen et al., 2004). Cl-rich fuels, such as wheat, rice,
141 brassica, etc., present limited interaction between the inorganic Cl and the proton
142 donating sites, thus, leading to lower Cl percentage release (Díaz-Ramírez et al.,
143 2014). The addition of sludges (typically rich in sulfur) modifies the chemistry involved
144 due to the reaction between KCl and sulfur. Thus, a total removal of Cl from the fly
145 ashes is theoretically possible if sulfur exists in sufficient amounts to react with all KCl
146 present (Equation 2, (Vainio et al., 2013)).



148 In the literature, it is also suggested that adding sludges may be beneficial for
149 inhibiting Cl deposits formation due to the following mechanisms (Åmand et al., 2006):

- 150 • Sulphur in the sludges may react with potassium, producing sulphate and
151 gaseous hydrogen chloride;

- 152 • Potassium chloride may be removed by condensation on fly ash particles
153 added with the sludge;
- 154 • Potassium in gaseous phase may react with aluminosilicates present in the
155 sludges;
- 156 • The deposits may be mechanically removed by the increased ash flows
157 caused by the sludges.

158 Thus, with sludge addition it can be expected a decrease of Cl emissions in the
159 solid phase and an increase of Cl emissions in the gaseous phase (Åmand and
160 Leckner, 2004) (HCl, e.g. equation 2). Nonetheless, if the sludges are rich in Ca, Cl
161 retention on ashes might increase while HCl concentration in the exhaust gases
162 decreases. These aspects need to be characterized and studied experimentally.

163 In this work, the co-combustion process of RFB from eucalyptus with primary
164 sludge (up to 5%wt) and secondary sludge (up to 10%wt) from wastewater treatment
165 was characterized. The sludge resulted from the wastewater treatment in the pulp and
166 paper industry. The influence of the addition of sludge on the overall process and on
167 the exhaust gases composition, with emphasis on Cl emissions, namely present in the
168 solid phase (fly ashes) and in the gaseous phase (HCl), and NO_x emissions, was
169 evaluated. The objective was to properly characterize the impact of the integration of
170 this energy valorization solution for the sludges, on the solids and exhaust gases
171 emissions during the co-combustion operation.

172

173 **2. Experimental work**

174 The experimental infrastructure used in this work includes a pilot-scale bubbling
175 fluidized bed (BFB) reactor with a combustion chamber of 0.25m diameter and 2.3m
176 height made of AISI 310SS. This infrastructure was previously used for gasification
177 works (Pio et al., 2018, 2017) but was properly updated for the co-combustion of RFB
178 and sludges. The general layout of the updated experimental infrastructure is shown in
179 Figure 1. The bottom bed of the reactor consists of 20kg of sand (98.3%wt. SiO₂

180 content)) with particle size in range 0.250 mm to 1.00 mm; the bottom bed of the
181 reactor has a static height of around 0.24m above the primary air (fluidizing air)
182 injectors. At typical operating conditions, the expanded (fluidized) bed height level is
183 approximately 0.30m above the distributor plate; the fluidizing bed height level can be
184 controlled by the discharge bed level at port C in Figure 1. The fluidized bed was
185 operated at atmospheric pressure and in bubbling regime, with superficial gas velocity
186 of around 0.28 to 0.30 m/s (depending on the operating conditions), and with average
187 bed temperatures in the range of 800 to 850 °C. The total combustion air was
188 maintained at 250 NL/min, distributed in 80% primary air (fluidization) and 20%
189 secondary air, in order to maintain the bottom bed and freeboard hydrodynamic
190 conditions. The stoichiometry conditions of the combustion process were controlled by
191 continuously monitoring the O₂ concentration in the exhaust gases, and through proper
192 adjustment of the biomass feed, which was maintained between 3 and 4 kg/h.

193 The biomass fuel used included distinct types of chipped RFB derived from
194 eucalyptus (*eucalyptus globulus*), different types of pellets produced from distinct
195 fractions of RFB from eucalyptus (branches with leaves, bark, etc.), and mixtures of
196 these types of RFB with primary (up to 5% wt.) and secondary (up to 10% wt.) sludges
197 resulting from wastewater treatment processes in the pulp and paper industry. The
198 pelletizing process of the RFB from eucalyptus was performed to increase the
199 uniformity of the physical characteristics of the fuel and improve the fuel feeding
200 regularity. The RFB from eucalyptus resulted from two different operations, namely
201 from forestry operations, as for example trees logging, and was named eucalyptus RFB
202 type A, and from industrial operations in the context of the pulp and paper industry,
203 namely woodchip production from eucalyptus logs, and was named eucalyptus RFB
204 type B. Both types of RFB were chipped, dried at atmospheric conditions and sieved to
205 a particle size below 5 mm. All the types of biomass were characterized in terms of
206 properties with interest for thermochemical conversion of biomass (proximate and

207 ultimate analysis, and heating value), as shown in Table 1. Some types of biomass
208 were characterized in terms of inorganics composition, as shown in Table 2.

209 The operating conditions during the combustion in the pilot-scale reactor were
210 characterized, namely the biomass fuel feed rate, air feed rate, temperature and
211 pressure along the reactor and gas composition at the exit. Table 3 shows information
212 regarding the operating conditions and the respective reference of the experiments
213 performed in this work.

214 The monitoring of the operating conditions was performed according to the
215 following methodologies:

- 216 1) Characterization of the exhaust gases:
 - 217 a) O₂ concentration determination in a paramagnetic analyzer (ADC-700);
 - 218 b) H₂O, O₂, CO, CO₂, CH₄, NO, SO₂ and HCl determination through heated
219 sampling and analysis (180°C) with measuring principle by FTIR (Gasmeter
220 CEM-II);
 - 221 c) Total particles concentration determination through isokinetic sampling in
222 quartz filters and their chemical characterization (Cl, Na, K and Ca). The
223 isokinetic sampling for particle concentration determination was performed
224 downstream of a cyclone and, in some cases, downstream of a bag filter
225 located after the cyclone. The content of Cl, K, Na and Ca in the particles
226 present in the exhaust gases (thinner fly ashes) is determined in terms of
227 the content of soluble inorganic ions (Cl⁻, K⁺, Ca²⁺ and Na⁺) by ion
228 chromatography in liquid phase according to the procedure described by
229 Calvo et al., in (Calvo et al., 2013).
- 230 2) Characterization of bottom bed ash and fly ash deposited in different locations
231 of the combustion system;
 - 232 a) Determination of chemical elements content (Cl, Na, K, Ca, Mg, Al, Mn and
233 P) was performed in an external laboratory (acid digestion followed by
234 Inductively Coupled Plasma Mass Spectrometry (ICP-MS) analysis).

235

236 3. Results and discussion

237 This section includes results regarding the combustion experiments performed,
238 namely, reactor temperature profiles (along time and longitudinal), combustion exhaust
239 gas composition profiles along time (CO_2 , H_2O , HCl , NO , CO and SO_2), chemical
240 composition (Cl , Na , K and Ca) of fly ash present in the exhaust gases, chemical
241 composition (Cl , Na , K , Ca , Mg , Al , Mn and P) of bottom bed ashes and of fly ashes
242 deposited in surfaces along the combustion system.

243

244 3.1. Temperature profiles

245 The evolution of temperature with time in different locations along the reactor
246 during the combustion of the different mixtures of biomass follows a similar pattern and
247 shows steady-state conditions of operation. These conditions were observed when
248 using only RFB from eucalyptus or mixtures of this biomass with primary (up to 5%wt)
249 and secondary sludge (up to 10%wt) (Figure 2). The temperature stability, despite the
250 fuel mixtures variability and feeding irregularities caused by the heterogeneous
251 physical characteristics of the RFB, is justified based on the recognized suitable mass
252 and energy transfer characteristics provided by the BFB operation regime (Knoef,
253 2005; Loo and Koppejan, 2008; Tarelho et al., 2011). The bed material allows the
254 absorption, storage and release of thermal energy and its mixing contributes to the
255 existence of uniform temperature in the bottom bed section. Consequently, the
256 biomass is rapidly converted after being fed to the reactor, due to the high heat
257 transfer. In this work, the bed temperature was maintained between 800 and 850°C.

258 The longitudinal temperature profile for the different combustion experiments
259 performed is shown in Figure 3. It is observed that the temperature increases from the
260 inside of the bed to the freeboard zone located immediately above the bed, where the
261 biomass is fed. The maximum temperature is observed close to the secondary air
262 injection. Above this region the temperature decreases with height due to heat losses

263 through the reactor walls, convection with the flue gas and the existence of a heat
264 exchanger (liquid water with a flow rate of 0.6 L/min) located 1 m above the distributor
265 plate (Figure 1). Similar to the observation performed regarding the temperature
266 profiles along time, it was observed that the introduction of sludge mixed with RFB did
267 not cause major changes in the longitudinal temperature profile.

268

269 3.2. Gas composition profiles

270 In this section, it is analyzed the typical concentration profile along time of different
271 gaseous species (CO_2 , H_2O , HCl , NO , CO and SO_2) present in the exhaust gases,
272 during the combustion experiments with different biomass mixtures (Table 3).

273

274 3.2.1. CO_2 and H_2O

275 In Figure 4, it can be observed typical CO_2 and H_2O concentration profiles for the
276 exhaust gases. It can be observed that both CO_2 and H_2O show small fluctuations with
277 time which can be justified by irregularities in the biomass feeding rate and the
278 heterogeneous physical and chemical characteristics of the biomass mixtures used.
279 Nonetheless, for long periods of operation, it can be assumed that the system was
280 operating in steady-state conditions in terms of CO_2 and H_2O concentration. CO_2
281 concentration was typically between 12 and 17%v (dry gas), which are typical values of
282 industrial combustion systems (Loo and Koppejan, 2008). The addition of primary and
283 secondary sludge did not cause any noticeable change in the CO_2 and H_2O
284 concentration profiles.

285

286 3.2.2. HCl

287 The HCl concentration profiles along time (Figures 5 and 6) show a distinct
288 behavior from the other chemical species (e.g., CO_2 , H_2O) analyzed. While these
289 species show a concentration that fluctuate around an average value, the HCl
290 concentration increases immediately after the introduction of biomass until attaining a

291 maximum value. Afterwards, HCl concentration decreases with time until reaching a
292 value that changes only in minor amounts with time. This behavior is more evident in
293 experiments with sludge addition. For these experiments, the addition of sludge to the
294 feedstock mixture caused an immediate decrease of HCl concentration in the
295 combustion flue gases (see Figure 5). This can be justified by the sludges high content
296 in ashes rich in CaO (Tables 1 and 2), which acts as adsorbent for acid species such
297 as HCl. In fact, the addition of Ca is recognized as an effective measure for HCl
298 removal in combustion systems (Xie and Ma, 2014). Therefore, sludge addition seems
299 to promote a decrease of the HCl concentration.

300 Despite the analogous conditions of operation obtained for the different combustion
301 experiments performed (e.g. Figures 2,3 and 4), it is observed that the HCl
302 concentration presents significant differences between experiments (Figure 6). On one
303 hand, this can be justified by the distinct Cl content present in each type of biomass
304 used as a feedstock (Table 1). On the other hand, it seems that lower stoichiometric
305 ratios (assumed by lower O₂ concentration in the combustion exhaust gases) tends to
306 contribute to higher HCl concentration in the exhaust gases, being that for the same
307 fuel mixture and bed temperature, lower HCl concentration values were found for lower
308 O₂ concentration in the exhaust gases (e.g. ELP-5 #2 and ELP-5 #4). This needs to be
309 investigated in future works.

310 It was also observed an effect of the operation time on the concentration of HCl in
311 the exhaust gases (Figure 5), i.e., with the increase of operation time, the concentration
312 of HCl in the exhaust gases tended to decrease. This effect might be related to the fact
313 that at the end of each combustion experiment the reactor bed was replaced by a new
314 sand bed. Thus, each experiment started with a clean bed without biomass/sludge
315 ashes. Therefore, it is reasoned that the concentration of HCl might be influenced by
316 the equilibrium between ash accumulation in the bottom bed and their capacity to
317 adsorb HCl. This effect was particularly relevant during combustion experiments where
318 sludge was included in the biomass mixture used as feedstock; the sludge promoted a

319 higher introduction of Ca compounds in the reactor, and thus increased the capacity of
320 the ashes to adsorb HCl.

321

322 3.2.3. NO

323 In Figures 7 and 8, it can be observed the NO concentration for the different
324 combustion experiments performed and its relation with the primary and secondary
325 sludges addition. The addition of secondary sludge caused a major increase in NO
326 concentration during the combustion of eucalyptus RFB type A (Figure 7 (a)). This can
327 be justified by the difference between the nitrogen content present in the secondary
328 sludges in comparison to the RFB from eucalyptus (Table 1). Analogous results were
329 obtained for eucalyptus RFB type B (EL-5, EL-10 and EL-10#2). The addition of
330 secondary sludge caused only a slight increase in the average NO concentration
331 during the combustion of pellets from eucalyptus bark (Pellets A and A*), however, it
332 led to the increase of the fluctuation of the NO concentration value (Figure 7 (b)). The
333 addition of secondary sludge did not cause noticeable changes in NO concentration
334 during combustion experiments with pellets from eucalyptus branches (Pellets E,
335 Figure 7 (c)). This can be justified by the already relatively high nitrogen content
336 present in this type of biomass (Table 1). The addition of primary sludge (up to 5%wt)
337 does not seem to promote any major change in the concentration of NO for all the
338 experiments performed (Figure 7 (d)).

339 Thus, in some cases, it was observed that the addition of secondary sludge
340 promoted an increase in NO concentration in the exhaust gases; however, in general, it
341 was not observed a significant difference between the NO concentration values in
342 experiments performed without sludges addition or with sludges addition in the referred
343 mass percentages. Typically, it was observed that the nitrogen content of the biomass
344 has direct influence on the NO concentration in the exhaust gases. NO concentration
345 values expressed as NO₂ (at 6%v O₂, dry gas) were typically between 215 mg/Nm³ and
346 433 mg/Nm³. The highest values were found during combustion experiments with

347 pellets from eucalyptus branches, which is justified by the higher nitrogen content
348 present in this biomass (Table 1). For comparison, the values obtained for the NO
349 concentration in these experiments were plotted against the ELV referred in the Best
350 Available Technologies (BAT) reference document for Large Combustion Plants (IPPC
351 2016, 2016) (180 mg/Nm³, 6% O₂) in Figure 8. It is observed that the experimental
352 values obtained are always above the referred limit.

353

354 3.2.4. CO

355 In general, it is observed that the concentration of CO in the exhaust gases is
356 below the emission limit value (ELV) (500 mg/Nm³, 11% O₂, Figure 9 (a)) imposed for
357 biomass boilers in the Portuguese legislation (in Portaria n.º 677/2009 (Governo de
358 Portugal, 2009), Portaria n.º 190-B/2018 (Governo de Portugal, 2018) does not include
359 CO ELVs). Nonetheless, during some experiments the CO concentration value
360 exceeded the ELV (e.g., EL-10# 2, Figure 9 (b)). This is related to significant biomass
361 feeding fluctuations caused by the heterogenous physical characteristics of the
362 biomass used as a feedstock in these experiments. Sludge addition did not promote
363 any visible change in CO concentration.

364

365

366 3.2.5. SO₂

367 It is observed that SO₂ concentration values are relatively low (Figure 10), which
368 results from the relatively low concentration of sulfur present in the biomass used as a
369 feedstock (Table 1). It is also observed that the addition of sludge did not cause any
370 significant change on the SO₂ concentration profiles, even though the secondary
371 sludges have higher sulfur content than all the types of RFB from eucalyptus tested.
372 This behavior may result from the fact that the sludge incorporation (up to 10%wt) is
373 not high enough to influence SO₂ concentration in the exhaust gases. Furthermore,
374 these sludges have a high Ca content, which can cause retention of SO₂ on ashes

375 (Vainio et al., 2013). The highest concentration value of SO₂ found was 17.2 mg/Nm³
376 (dry gas, 11% O₂) during experiment EL-10, which is significantly lower than the ELV
377 (500 mg/Nm³, 11%O₂, Figure 10) referred for biomass boilers in the Portuguese
378 legislation (in Portaria n.º 677/2009 (Governo de Portugal, 2009), Portaria n.º 190-
379 B/2018 (Governo de Portugal, 2018) does not stipulate O₂ reference value for SO₂
380 concentration ELV).

381

382 3.3. Particulate matter analysis

383 3.3.1. Fly ashes in the exhaust gases

384 In this section, the average particle concentration and composition (Cl, K, Ca, and
385 Na) in the exhaust gases during the co-combustion experiments performed is
386 presented and analyzed.

387 The average particle concentration in the exhaust gases during each combustion
388 experiment performed is shown in Figure 11. It is typically observed lower particle
389 concentration in experiments with chipped RFB from eucalyptus (EL-0, EL-5, EL-10
390 and EL-10 #2) than in experiments performed with pellets produced from fractions of
391 RFB from eucalyptus (EL-0 #2, EL-10 #3, EL-10 #4, EL-10 #5, EL-10 #6, EL-10 #7, EL-
392 10 #8, ELP-5, ELP-5 #2, ELP-5 #3 and ELP-5 #4). In part, this is justified by the lower
393 ash content of the chipped RFB (Table 1); bark and leaves typically have higher ash
394 content than fractions of wood. In fact, combustion experiments of pellets from
395 eucalyptus bark (EL-10 #6, EL-10 #8 and ELP-5 #3) and pellets from eucalyptus
396 branches (Pellets E, EL-10 #7, ELP-5 #2 and ELP-5 #4) presented particle
397 concentration significantly higher than other combustion experiments with other types
398 of pellets. Nonetheless, the co-combustion experiment performed with the biomass
399 feedstock with highest ash content (Pellets C, EL-10 #5) did not present higher fly ash
400 concentration in the exhaust gases. Thus, other factors apart from the ash content of
401 the biomass may have influenced the formation of fly ash, such as the physical

402 characteristics of the pellets (e.g., density and hardness) and the chemical composition
403 of the ashes (Sippula, 2010). Future works should address this behavior.

404 Two main observations can be made regarding the effect of the addition of primary
405 and secondary sludge on the particle concentration in the exhaust gases. In some
406 cases, the sludge addition seems to promote a small increase of the particle
407 concentration (e.g. EL-10 #3 and ELP-5), which is justified by the higher ash content
408 present in the sludge in comparison to the RFB from eucalyptus (Table 1). In other
409 cases, it was observed the opposite, i.e., the decrease of particles concentration after
410 the addition of sludge (e.g. EL-10 #6, EL-10 #7 and ELP-5 #3). Nonetheless, in these
411 experiments, when the sludge feeding ended, the particles concentration continued to
412 decrease. The justification for this phenomenon may be related to the high content of
413 Ca present in the ashes retained in the bed and on the exhaust duct, which may have
414 prevented the formation of thinner fly ashes. In fact, the major components present in
415 the fly ashes from the exhaust gases are Cl and K (Figure 12), whereas Ca was found
416 as the major element in the composition of bottom bed ashes and ashes deposited in
417 inner surfaces of the combustion system (Figure 15). This will be discussed in the
418 following Section 3.3.2.. Similar results were observed in other works regarding co-
419 combustion of RFB with sludge from the pulp and paper industry (Vainio et al., 2013).

420 K concentration (Figure 12) in the fly ashes was typically higher for experiments
421 with pellets from eucalyptus bark (e.g., Pellets A*, EL-10 #6, EL-10 #8 and ELP-5 #3)
422 and pellets from eucalyptus branches (Pellets E, EL-10 #7, ELP-5 #2 and ELP-5 #4).
423 Furthermore, a linear correlation between K and Cl concentration was found for the
424 particle matter in the exhaust gas (Figure 13 (a)). This relation is close to the mass
425 ratio 1:0.91 for K:Cl in the compound KCl, which indicates that a significant part of Cl in
426 the fly ashes present in the exhaust gases might be in the form of KCl, as suggested by
427 some other works (Loo and Koppejan, 2008).

428 Ca and Na concentration values in the fly ashes present in the exhaust gases
429 (Figure 12) are significantly lower than the K and Cl concentration values. Furthermore,

430 even though Ca has the capacity to remove Cl in gaseous effluents (Partanen et al.,
431 2005), only a weak relationship between Ca and Cl in the fly ashes was observed
432 (Figure 13 (b)). The relatively low concentration value found for Ca in the fly ashes is in
433 contrast with that found for the bottom bed ashes and ashes deposited in inner
434 surfaces of the BFB reactor (Figure 15, Section 3.3.2); in fact, Ca is the main alkali
435 element present in the ashes from the RFB and sludges used (Table 2). The Na
436 concentration in the fly ashes present in the exhaust gases is lower than Ca, however,
437 it is observed a stronger linear relation between the mass concentration of Na and Cl
438 (Figure 13 (c)). Nonetheless, this relation is significantly lower than the mass ratio of
439 1:1.5 for Na:Cl present in the compound NaCl.

440 In summary, it is observed that the mass concentration of chemical elements in the
441 fly ashes sampled in the exhaust gases during the combustion experiments shows the
442 following decreasing order of abundance: Cl > K > Ca > Na.

443 In Figure 14, it is shown the contribution from the gaseous phase (measured as
444 HCl) and the particulate phase (fly ashes present in the exhaust gases) to the emission
445 of Cl during the combustion experiments. It is observed that the concentration of Cl
446 (quantified as the chlorine ion Cl⁻, by ion chromatography) in the solid phase
447 (associated to fly ashes in the exhaust gases and denoted as Cl-particles in Figure 14)
448 is higher than in the gaseous phase (associated to HCl and denoted as Cl-HCl in
449 Figure 14) for the combustion experiments performed. It is also observed that the Cl
450 emissions for both solid and gas phases are related to the Cl content in the biomass
451 mixture used as feedstock. For example, experiments with pellets from eucalyptus bark
452 (e.g. Pellets A*, EL-10 #6, EL-10 #8 and ELP-5 #3) or eucalyptus branches (Pellets E,
453 EL-10 #7, ELP-5 #2 and ELP-5 #4), which have a high Cl content (Table 1), caused
454 higher average emissions of Cl in both solid and gaseous phase (Figure 14). Similar to
455 the observations made regarding Cl concentration in the gaseous phase (HCl),
456 discussed in the previous Section 3.2.2, the addition of sludge seems to have caused a
457 decrease of Cl concentration in the fly ashes present in the exhaust gases (e.g. EL-10

458 #2, EL-10 #6, EL-10 #7, ELP-5 and ELP-5 #3), which can be related to the Ca present
459 in the sludge ashes and the respective adsorption of Cl by heavier particles retained in
460 the BFB, e.g., in the bottom bed; however, some exceptions were observed that must
461 be accounted (EL-10 #3, EL-10 #4 and EL-10 #5). This phenomenon should be
462 addressed in future works.

463

464 3.3.2. Bottom bed ashes and fly ashes deposited along the combustion system

465 In this section, results regarding the chemical characterization (Ca, K, Mg, P, Na,
466 Al, Mn and Cl) of samples of bottom bed ashes and fly ashes deposited along the
467 combustion system are presented and analyzed. The chosen locations of the
468 combustion system for sampling the ashes were the bottom bed surface layer, the
469 reactor walls above the distributor plate, a cold (liquid water cooling) deposition probe
470 located 2.2 m above the distributor plate, the bottom of the horizontal exhaust duct of
471 the reactor and the ash retained in the cyclone located downstream of the BFB reactor.
472 The ashes were sampled after the experiments with reference EL-10 #4, EL-10 #6, EL-
473 10 #7, ELP-5 #3 and ELP-5 #4 (Table 3); The average concentration values (Ca, K,
474 Mg, P, Na, Al, Mn and Cl) found are shown in Figure 15.

475 It is observed that Ca is present in significantly higher concentration in the different
476 ash samples than the other analyzed elements (Figure 15). This results from Ca being
477 the main chemical element present in the ashes for both RFB from eucalyptus and
478 sludges (Table 2). Regardless of the sampling location, the average concentration of
479 chemical elements on the ashes is by descending order of abundance:
480 $Ca > K > Cl > Mg > P > Na > Al > Mn$. This composition is distinct from that observed for the fly
481 ashes in the exhaust gases, where K and Cl were the main chemical elements (Figure
482 12). Nevertheless, K and Cl are still present in relatively high concentration in the
483 bottom bed ashes and deposited ashes along the reactor surfaces. These elements
484 are associated with corrosion processes (Davidsson et al., 2007; Hupa, 2012; Loo and
485 Koppejan, 2008; Nielsen et al., 2000; Vainio et al., 2013), thus, their retention in the

486 bottom bed ashes is desired. In fact, co-combustion of RFB with sludge from the pulp
487 and paper industry has been referred as beneficial to prevent corrosion from
488 compounds derived from Cl and K (Aho et al., 2010; Aho and Silvennoinen, 2004;
489 Åmand et al., 2006; Vainio et al., 2013), which could be related to the high Ca content
490 of the ashes.

491 The concentration of the analyzed chemical elements in the bottom bed ashes is
492 significantly lower than in the fly ashes deposited in other locations of the combustion
493 system. This is justified by the fact that even after the combustion process, the bottom
494 bed particle samples are composed mainly of the original sand (98.3%wt. SiO₂ content)
495 and silicon was not analyzed. Nonetheless, the sum of the average concentration of
496 the analyzed chemical elements on the particle samples collected at the surface layer
497 of the bottom bed is around 4.4%wt., which means that the sand from the bed is
498 enriched with typical elements from the ashes of the biomass.

499 Accordingly, it is observed a trend for the increase of the concentration of the
500 analyzed chemical elements with the increase of the distance to the distributor plate.
501 Furthermore, the maximum concentration value for these analyzed chemical elements
502 was typically found in the ashes collected on the exhaust duct or the cyclone. Some
503 exceptions observed are: experiment EL-10 #4 where Cl concentration decreased from
504 the surface of the bed to the exhaust duct and experiment EL-10 #7 where the highest
505 Cl concentration value was found in the ashes collected in the deposition probe located
506 at the top of the combustion chamber. In fact, the maximum average Cl concentration
507 value was found in the ashes collected on the deposition probe. It was also found that
508 the average sum of chemical elements analyzed (Na, K, Mg, Al, Mn, P, Ca and Cl) in
509 the ashes collected in the deposition probe and exhaust duct was 40.2% and 44.6%wt
510 db, respectively. This shows that the fly ashes deposited along the reactor are
511 significantly enriched in typical elements of biomass inorganics, which in industrial
512 scenarios may lead to relevant corrosion issues.

513 Thus, the excess Ca introduced through the sludge addition seems to have caused
514 a higher retention of Cl in the bottom bed ashes and fly ashes deposited on solid
515 surfaces exposed to the exhaust gases. This might justify the reduction in HCl
516 concentration in the exhaust gases observed with the addition of sludge, which was
517 previously discussed in Section 3.2.2.

518

519 **4. Conclusions**

520 The objective of this work was the evaluation of the co-combustion process of RFB
521 from eucalyptus with primary (up to 5%wt) and secondary (up to 10%wt) sludge from
522 the pulp and paper industry in a pilot-scale BFB reactor, with emphasis on NO and Cl
523 related emissions.

524 The continuous monitoring of the operating parameters, such as temperature and
525 exhaust gas composition along time in the BFB, during the co-combustion process of
526 the different mixtures of RFB and sludge, showed that the reactor was operating under
527 steady-state conditions.

528 Regarding the composition of the exhaust gases, a continuous HCl concentration
529 decrease with time until reaching an almost constant value was observed during the
530 combustion process. This behavior can be related to the Cl retention promoted by the
531 alkaline elements present in the biomass, such as Ca and K. In fact, sludge addition
532 typically caused a decrease in the concentration of HCl in the exhaust gases, which
533 can be related to the high content of alkaline elements present in the sludge (e.g., Ca).

534 Regarding NO concentration in the exhaust gases, it was observed that it is mainly
535 influenced by the characteristics of the feedstock used. It was also observed that the
536 addition of sludge to RFB with low N content (e.g. eucalyptus wood chips) caused a
537 significant increase in NO concentration during the combustion process. On the other
538 hand, addition of sludge to RFB with high N content (e.g., eucalyptus bark) did not
539 seem to promote any noticeable increase in the NO concentration. For all the
540 combustion experiments performed, the NO concentration (expressed as NO₂) values

541 found in the exhaust gases met the stipulated ELV for biomass furnaces in the
542 Portuguese legislation (Portaria 677/2009 (Governo de Portugal, 2009)), but are above
543 the ELV indicated in the BAT reference document for Large Combustion Plants (IPPC
544 2016, 2016).

545 Regarding CO concentration in the exhaust gases, it was observed that it is
546 immensely influenced by the regularity of the biomass feeding and that sludge
547 introduction in the fuel mixture did not seem to promote any noticeable changes.
548 Furthermore, by using an adequate control of the feeding conditions and an
549 appropriate stoichiometric ratio, it was possible to meet the stipulated ELV for CO
550 concentration in the exhaust gases from biomass furnaces according to the Portuguese
551 legislation (Portaria 677/2009 (Governo de Portugal, 2009)).

552 Regarding SO₂ concentration in the exhaust gases, it was observed that this value
553 was significantly lower than the ELV stipulated for biomass furnaces in the Portuguese
554 legislation (Portaria 677/2009 (Governo de Portugal, 2009)). Furthermore, sludge
555 addition to the fuel mixture did not cause a noticeable increase in the concentration of
556 SO₂.

557 Regarding the fly ashes particles emitted with the exhaust gases, it was observed
558 that Cl and K were the major inorganic chemical elements present in the fly ashes. It is
559 reasoned that these two elements might be in the form of KCl, due to the observation
560 of a linear relation between Cl and K with a mass ratio K:Cl close to 1:0.91. It was also
561 observed that the mass of Cl emitted in the particulate phase was significantly higher
562 than that emitted in the gas phase as HCl.

563 The characterization of the bottom bed ashes and ashes deposited in inner
564 surfaces along the combustion system, considering the chemical elements Ca, K, Mg,
565 P, Na, Al, Mn and Cl, showed that the average concentration of chemical elements in
566 the sampled ashes is (by decreasing order of abundance)
567 Ca>K>Cl>Mg>P>Na>Al>Mn, regardless of the location of the sampling point. This
568 knowledge is relevant to understand the potential negative effects that ashes can

569 cause on combustion equipment, such as slagging and fouling, and upon the
570 environment after emission to the atmosphere.

571 Thus, this work demonstrates the potential of the co-combustion of RFB from
572 eucalyptus with primary or secondary sludge in BFB. Except specific cases, it was not
573 found a significant increase of NO, CO or HCl emissions with the addition of sludge to
574 the fuel mixture. In fact, the addition of sludge typically promoted a decrease of HCl
575 concentration in the exhaust gases, which can be related to Cl retention in Ca rich
576 ashes. Nonetheless, for RFB from eucalyptus with low N content, the addition of sludge
577 to the fuel mixture led to higher NO emissions. Furthermore, the high inorganic content
578 present in the sludge can originate a significant increase in the amount of ash
579 production. The accumulation of these ashes along time and along the combustion
580 system (e.g. heat exchangers), can promote operational problems, such as the
581 decrease of the process efficiency, increase of maintenance operation needs and
582 equipment damage. This must be investigated in future works.

583

584 **Acknowledgments**

585 The authors acknowledge the Portuguese Foundation for Science and Technology
586 (FCT) for the financial support provided through project PTDC/AAC-AMB/ 116568/2010
587 (Project n.º FCOMP-01-0124-FEDER-019346) “BiomAshTech - Ash impacts during
588 thermo-chemical conversion of biomass”. Thanks are due for the financial support to
589 CESAM (UID/AMB/50017/2019), to FCT/MCTES through national funds, and the co-
590 funding by the FEDER, within the PT2020 Partnership Agreement and Compete 2020,
591 and Compete 2020. The authors also acknowledge the FCT and The Navigator
592 Company for providing financial support to the PhD scholarship granted to Daniel Pio
593 (ref. PD/BDE/128620/2017).

594

595 **References**

596 Aho, M., Silvennoinen, J., 2004. Preventing chlorine deposition on heat transfer

- 597 surfaces with aluminium-silicon rich biomass residue and additive. *Fuel* 83, 1299–
598 1305. <https://doi.org/10.1016/j.fuel.2004.01.011>
- 599 Aho, M., Yrjas, P., Taipale, R., Hupa, M., Silvennoinen, J., 2010. Reduction of
600 superheater corrosion by co-firing risky biomass with sewage sludge. *Fuel* 89,
601 2376–2386. <https://doi.org/10.1016/j.fuel.2010.01.023>
- 602 Åmand, L.E., Leckner, B., 2004. Gaseous emissions from co-combustion of sewage
603 sludge and coal/wood in a fluidized bed. *Fuel* 83, 1803–1821.
604 <https://doi.org/10.1016/j.fuel.2004.01.014>
- 605 Åmand, L.E., Leckner, B., Eskilsson, D., Tullin, C., 2006. Deposits on heat transfer
606 tubes during co-combustion of biofuels and sewage sludge. *Fuel* 85, 1313–1322.
607 <https://doi.org/10.1016/j.fuel.2006.01.001>
- 608 Calvo, A.I., Tarelho, L.A.C., Teixeira, E.R., Alves, C., Nunes, T., Duarte, M., Coz, E.,
609 Custodio, D., Castro, A., Artiñano, B., Fraile, R., 2013. Particulate emissions from
610 the co-combustion of forest biomass and sewage sludge in a bubbling fluidised
611 bed reactor. *Fuel Process. Technol.* 114, 58–68.
612 <https://doi.org/10.1016/j.fuproc.2013.03.021>
- 613 Chen, T., Lei, C., Yan, B., Li, L., 2019. Analysis of heavy metals fixation and associated
614 energy consumption during sewage sludge combustion: Bench scale and pilot
615 test. *J. Clean. Prod.* 229, 1243–1250. <https://doi.org/10.1016/j.jclepro.2019.04.358>
- 616 Davidsson, K.O., Åmand, L.E., Leckner, B., Kovacevik, B., Svane, M., Hagström, M.,
617 Pettersson, J.B.C., Petterson, J., Asteman, H., Svensson, J.E., Johansson, L.G.,
618 2007. Potassium, chlorine, and sulfur in ash, particles, deposits, and corrosion
619 during wood combustion in a circulating fluidized-bed boiler. *Energy and Fuels* 21,
620 71–81. <https://doi.org/10.1021/ef060306c>
- 621 Díaz-Ramírez, M., Frandsen, F.J., Glarborg, P., Sebastián, F., Royo, J., 2014.
622 Partitioning of K, Cl, S and P during combustion of poplar and brassica energy
623 crops. *Fuel* 134, 209–219. <https://doi.org/10.1016/j.fuel.2014.05.056>
- 624 Hao, Z., Yang, B., Jahng, D., 2018. Combustion characteristics of biodried sewage

- 625 sludge. *Waste Manag.* 72, 296–305.
- 626 <https://doi.org/10.1016/j.wasman.2017.11.008>
- 627 Hupa, M., 2012. Ash-related issues in fluidized-bed combustion of biomasses: Recent
628 research highlights. *Energy and Fuels* 26, 4–14. <https://doi.org/10.1021/ef201169k>
- 629 IPCC 2016, 2016. Large Combustion Plants, Integrated Pollution Prevention and
630 Control 976. <https://doi.org/10.1016/j.jhazmat.2006.07.037>
- 631 Jensen, P., Frandsen, F., Dam-Johansen, K., Sander, B., 2000. Experimental
632 investigation of the transformation and release to gas phase of potassium and
633 chlorine during straw pyrolysis. *Energy & Fuels* 14, 1280–1285.
634 <https://doi.org/10.1021/ef000104v>
- 635 Johansen, J.M., Jakobsen, J.G., Frandsen, F.J., Glarborg, P., 2011. Release of K, Cl,
636 and S during pyrolysis and combustion of high-chlorine biomass. *Energy and
637 Fuels* 25, 4961–4971. <https://doi.org/10.1021/ef201098n>
- 638 Kijo-Kleczkowska, A., Środa, K., Kosowska-Golachowska, M., Musiał, T., Wolski, K.,
639 2016. Experimental research of sewage sludge with coal and biomass co-
640 combustion, in pellet form. *Waste Manag.* 53, 165–181.
641 <https://doi.org/10.1016/j.wasman.2016.04.021>
- 642 Knoef, H., 2005. Handbook of Biomass Gasification. BTG Group 2005:378.
- 643 Knudsen, J.N., Jensen, P.A., Dam-Johansen, K., 2004. Transformation and release to
644 the gas phase of Cl, K, and S during combustion of annual biomass. *Energy and
645 Fuels* 18, 1385–1399. <https://doi.org/10.1021/ef049944q>
- 646 Lith, S.C. Van, Jensen, P.A., Frandsen, F.J., Glarborg, P., 2004. Release of Inorganic
647 Elements During Wood Combustion. *Prepr. Pap.-Am. Chem. Soc., Div. Fuel
648 Chem* 49, 87–88.
- 649 Lokare S.S., 2008. A Mechanistic Investigation of Ash Deposition in Pulverized-coal
650 and Biomass Combustion. ProQuest.
- 651 Loo, S. Van, Koppejan, J., 2008. The Handbook of Biomass Combustion and Co-firing.
652 2008.

- 653 Meyer, T., Amin, P., Allen, D.G., Tran, H., 2018. Dewatering of pulp and paper mill
654 biosludge and primary sludge. *J. Environ. Chem. Eng.* 6, 6317–6321.
655 <https://doi.org/10.1016/j.jece.2018.09.037>
- 656 Nielsen, H.P., Frandsen, F.J., Dam-Johansen, K., Baxter, L.L., 2000. Implications of
657 chlorine-associated corrosion on the operation of biomass-fired boilers. *Prog.*
658 *Energy Combust. Sci.* 26, 283–298. [https://doi.org/10.1016/S0360-](https://doi.org/10.1016/S0360-1285(00)00003-4)
659 [1285\(00\)00003-4](https://doi.org/10.1016/S0360-1285(00)00003-4)
- 660 Olsson, J.G., Ja, U., Pettersson, J.B.C., 1997. Alkali Metal Emission during Pyrolysis of
661 Biomass. *Energy & Fuels* 11, 779–784. <https://doi.org/10.1021/ef960096b>
- 662 Partanen, J., Backman, P., Backman, R., Hupa, M., 2005. Absorption of HCl by
663 limestone in hot flue gases. Part I: The effects of temperature, gas atmosphere
664 and absorbent quality. *Fuel* 84, 1664–1673.
665 <https://doi.org/10.1016/j.fuel.2005.02.011>
- 666 Pio, D.T., Tarelho, L.A.C., Matos, M.A.A., 2017. Characteristics of the gas produced
667 during biomass direct gasification in an autothermal pilot-scale bubbling fluidized
668 bed reactor. *Energy* 120, 915–928. <https://doi.org/10.1016/j.energy.2016.11.145>
- 669 Pio, D.T., Tarelho, L.A.C., Pinto, R.G., Matos, M.A.A., Frade, J.R., Yaremchenko, A.,
670 Mishra, G.S., Pinto, P.C.R., 2018. Low-cost catalysts for in-situ improvement of
671 producer gas quality during direct gasification of biomass. *Energy* 165.
672 <https://doi.org/10.1016/j.energy.2018.09.119>
- 673 Portaria n.º190-B/2018. *Diário Da República*, 1.ª série, n.º125, 2 de julho 2018:2880–4.
- 674 Portaria n.º677/2009. *Diário Da República*, 1ª série, n.º119, 23 de junho 2009:4112–6.
- 675 Sippula, O., 2010. Fine particle formation and emission in biomass combustion, PhD
676 thesis, University of Eastern Finland 2010.
- 677 Strömberg, B., Björkman, E., 1997. Release of Chlorine from Biomass at Pyrolysis and
678 Gasification Conditions. *Energy & Fuels* 11, 1026–1032.
679 <https://doi.org/10.1002/9780470694954.ch102>
- 680 Sung, J.H., Back, S.K., Jeong, B.M., Kim, J.H., Choi, H.S., Jang, H.N., Seo, Y.C.,

- 681 2018. Oxy-fuel co-combustion of sewage sludge and wood pellets with flue gas
682 recirculation in a circulating fluidized bed. *Fuel Process. Technol.* 172, 79–85.
683 <https://doi.org/10.1016/j.fuproc.2017.12.005>
- 684 Tarelho, L.A.C., Neves, D.S.F., Matos, M.A.A., 2011. Forest biomass waste
685 combustion in a pilot-scale bubbling fluidised bed combustor. *Biomass and*
686 *Bioenergy* 35, 1511–1523. <https://doi.org/10.1016/j.biombioe.2010.12.052>
- 687 Vainio, E., Yrjas, P., Brink, A., Laurén, T., Kajolinna, T., Vesala, H., 2013. The fate of
688 chlorine, sulfur, and potassium during co-combustion of bark, sludge, and solid
689 recovered fuel in an industrial scale BFB boiler. *Fuel Process. Technol.* 105, 59–
690 68. <https://doi.org/10.1016/J.FUPROC.2011.08.021>
- 691 van Lith, S.C., Alonso-Ramírez, V., Jensen, P.A., Frandsen, F.J., Glarborg, P., 2006.
692 Release to the gas phase of inorganic elements during wood combustion. Part 1:
693 Development and evaluation of quantification methods. *Energy and Fuels* 20,
694 964–978. <https://doi.org/10.1021/ef050131r>
- 695 Viklund, P., 2013. Superheater corrosion in biomass and waste fired boilers
696 Characterisation , causes and prevention of chlorine-induced corrosion, PhD
697 thesis, KTH Royal Institute of Technology 2013.
- 698 Xie, Z., Ma, X., 2014. HCl emission characteristics during the combustion of eucalyptus
699 bark. *Energy and Fuels* 28, 5826–5833. <https://doi.org/10.1021/ef5009242>
- 700 Zhao, Z., Wang, R., Wu, J., Yin, Q., Wang, C., 2019. Bottom ash characteristics and
701 pollutant emission during the co-combustion of pulverized coal with high mass-
702 percentage sewage sludge. *Energy* 171, 809–818.
703 <https://doi.org/10.1016/j.energy.2019.01.082>
704
705
706

707 Table 1 – Characteristics of the different types of biomass used as feedstock in the
 708 combustion experiments in the pilot-scale BFB.

	Eucalyptus RFB		Pellets						Sludge	
	Type A	Type B	A	A*	B	C	D	E	Primary	Secondary
Proximate analysis (%wt, db)										
Moisture	11.4	11.8	7.7	10.2	8.3	8.9	8.3	7.9	11.3	20.0
Volatile matter	77.3	80.5	78.3	78.1	78.2	77.1	79.0	77.1	na	na
Fixed carbon	21.5	16.6	16.7	17.5	19.0	15.7	17.7	18.4	na	na
Ash	1.2	2.9	5.0	4.5	2.8	7.3	3.3	4.4	61.5	26.5
Ultimate analysis (%wt, db)										
Ash	1.2	2.9	5.0	4.5	2.8	7.3	3.3	4.4	61.5	26.5
C	49.1	48.2	44.4	46.4	50.6	48.2	50.9	51.4	32.4	36.7
H	6.5	6.2	5.4	5.7	6.2	6.2	6.1	6.1	4.2	5.0
N	0.1	<0.2	0.2	0.7	0.8	<0.2	0.9	1.4	0.5	2.2
S	nd	0.03	0.03	nd	nd	0.03	nd	nd	nd	0.4
O (by difference)	43.2	42.7	44.7	42.3	39.5	38.3	38.6	36.3	1.4	29.0
Cl	0.05	0.05	0.20	0.40	0.14	0.05	0.18	0.38	0.02	0.19

709 wb - wet basis; db - dry basis; np – not available; nd – not determined, below the detection limit of the method, 100 ppm wt.

710

711 Table 2 – Concentration of Ca, Na, K, Mg, Al, Mn and P in the ashes from the different
 712 types of biomass used as feedstock in the combustion experiments in the pilot-scale
 713 BFB

Ash elemental analysis	Pellets				Sludge	
	A*	B	D	E	Primary	Secondary
	Ppm wt., db					
Ca	8060	6960	7910	9480	245000	106166
Na	635	3920	396	952	4290	nd
K	3240	2750	2610	6310	291	1134
Mg	1730	668	546	1421	1800	1608
Al	367	41.9	63.3	61.2	313	869
Mn	219	139	157	99	168	nd
P	302	289	263	511	3450	2500

db – dry basis; nd – not determined.

714

715

716 Table 3 – Combustion experiments reference and respective operating parameters.

Experiment reference	Biomass (%wt.)	Type of RFB	Average bed temperature [°C]	O ₂ (%v, dry gas) in the exhaust combustion gases
EL-0	100% eucalyptus	Eucalyptus RFB type A	804	7.0
EL-0 #2	100% eucalyptus	Diverse pellets	821	8.1
EL-5	5% secondary sludge + 95% eucalyptus	Eucalyptus RFB type A	815	7.0
EL-10	10% secondary sludge + 90% eucalyptus	Eucalyptus RFB type A	810	6.2
EL-10 #2	10% secondary sludge + 90% eucalyptus	Eucalyptus RFB type B	825	7.4
EL-10 #3	10% secondary sludge + 90% eucalyptus	Pellets A	837	7.1
EL-10 #4	10% secondary sludge + 90% eucalyptus	Pellets B	848	7.2
EL-10 #5	10% secondary sludge + 90% eucalyptus	Pellets C	839	6.9
EL-10 #6	10% secondary sludge + 90% eucalyptus	Pellets A*	830	5.9
EL-10 #7	10% secondary sludge + 90% eucalyptus	Pellets E	828	6.0
EL-10 #8	10% secondary sludge + 90% eucalyptus	Pellets A*	836	4.5
ELP-5	5% primary sludge + 95% eucalyptus	Pellets D	837	8.0
ELP-5 #2	5% primary sludge + 95% eucalyptus	Pellets E	819	6.0
ELP-5 #3	5% primary sludge + 95% eucalyptus	Pellets A*	838	5.5
ELP-5 #4	5% primary sludge + 95% eucalyptus	Pellets E	820	7.9

717 Legend: Diverse pellets – Different pellets used during the combustion experiment, namely, commercial pine pellets (2h), pellets A (5h)
718 and pellets B (2h); Pellets A – Pellets from eucalyptus bark resulting from operations in the pulp and paper industry (sample 1); Pellets
719 A* - Pellets from eucalyptus bark resulting from operations in the pulp and paper industry (sample 2); Pellets B – Pellets from eucalyptus
720 branches, resulting from forest maintenance operations, with residual amounts of eucalyptus foliage; Pellets C – Pellets from powdered
721 eucalyptus chips (<1mm) Pellets D – Pellets resulting from eucalyptus RFB type A and type B and eucalyptus foliage; Pellets E – Pellets
722 from powdered eucalyptus branches.

723

Figure 1 – Layout of the experimental infrastructure with the pilot-scale BFB reactor. Dashed line — Electric circuit, Solid line — Pneumatic circuit, A - Primary air heating system, B - Sand bed, C - Bed solids level control, D - Bed solids discharge, E - Bed solids discharge silo, F - Propane burner system, G - Port for visualization of bed surface, H - Air flow meter (primary and secondary air), I - Control and command unit (UCC2), J - Biomass feeder, K - Water-cooled gas sampling probe, , N - Gas sampling pump, O - Gas condensation unit for moisture removal, Y – Computer based control and data acquisition system, Z - Exhaust duct; O₂ – Online paramagnetic analyzer for the determination of O₂ (ADC-700), FTIR – Online infrared analyzer for determination of H₂O, CO₂, CO, N₂O, NO, NO₂, SO₂, HCl, NH₃, CH₄, etc., HTSU – High Temperature Sampling Unit, UCD0, UCD1, UCD2 - Electro-pneumatic command and gas distribution units, UCE1 - Electronic command unit.

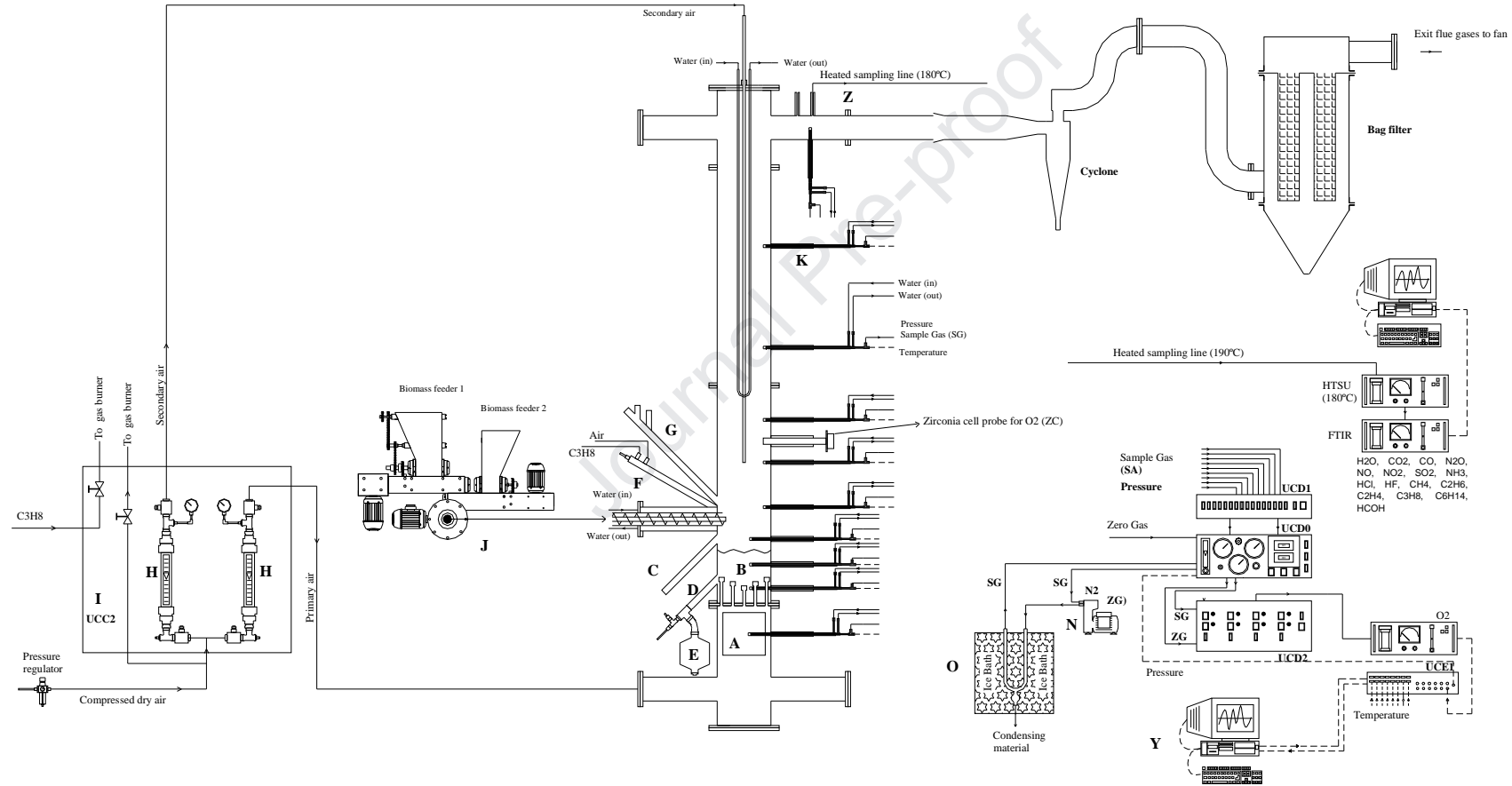
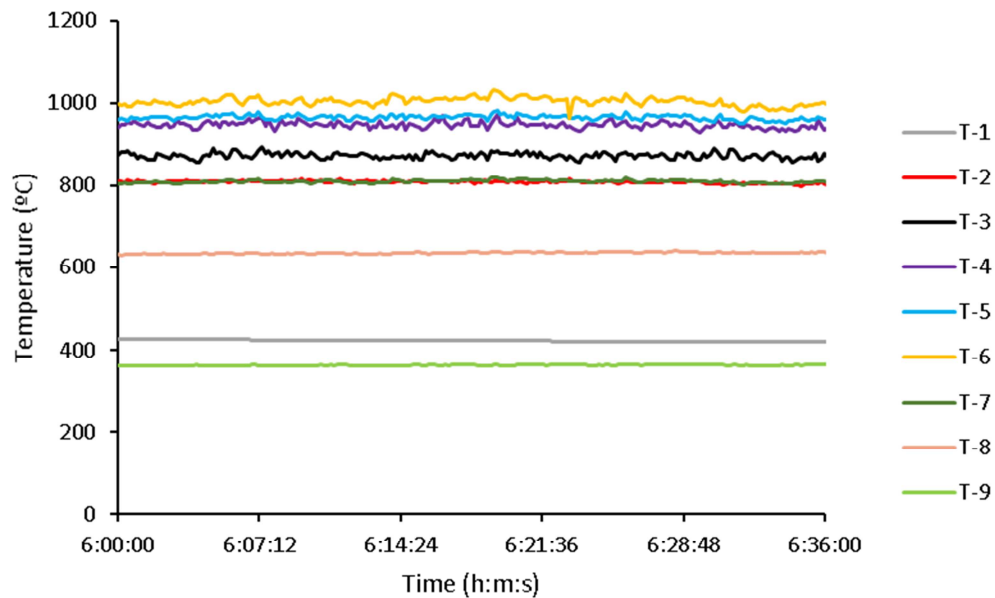
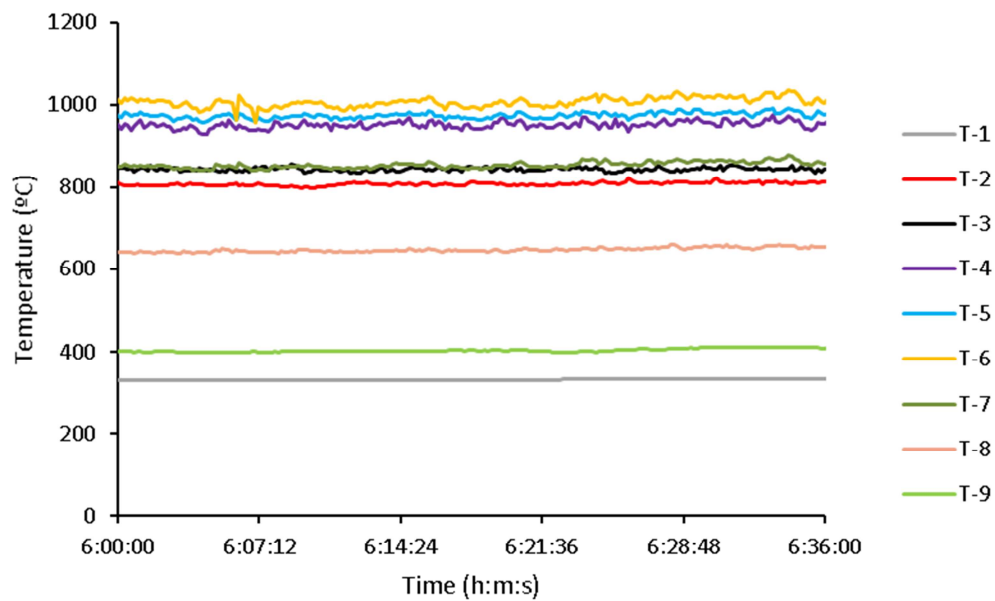


Figure 2 – Typical evolution of the temperature along time at different locations along the reactor height during the combustion experiments: (a) EL-0, (b) EL-10 and (c) ELP-5. Experiments reference according to Table 3. Temperature measurement locations above distributor plate: T1 – 0.05 m, T2 – 0.18 m, T3 – 0.30 m, T4 – 0.45 m, T5 – 0.66m, T6 – 0.86 m, T7 – 1.20 m, T8 – 1.68 m and T9 – 2.90 m.

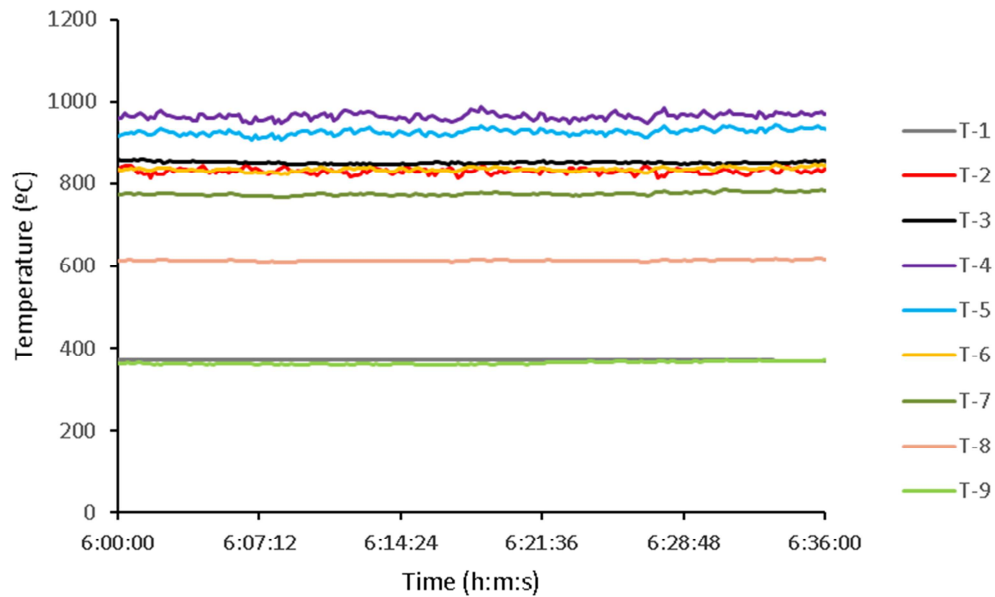


(a)



(b)

Figure 2 (continuation) – Example of the typical evolution of the temperature along time at different locations along the reactor height during the following combustion experiments: (a) EL-0, (b) EL-10 and (c) ELP-5. Experiments reference according to Table 3. Temperature measurement locations above distributor plate: T1 – 0.05 m, T2 – 0.18 m, T3 – 0.30 m, T4 – 0.45 m, T5 – 0.66 m, T6 – 0.86 m, T7 – 1.20 m, T8 – 1.68 m and T9 – 2.90 m.



(c)

Figure 3 – Longitudinal temperature profile in the BFB reactor during the biomass combustion experiments performed. Legend according to experiments references in Table 3.

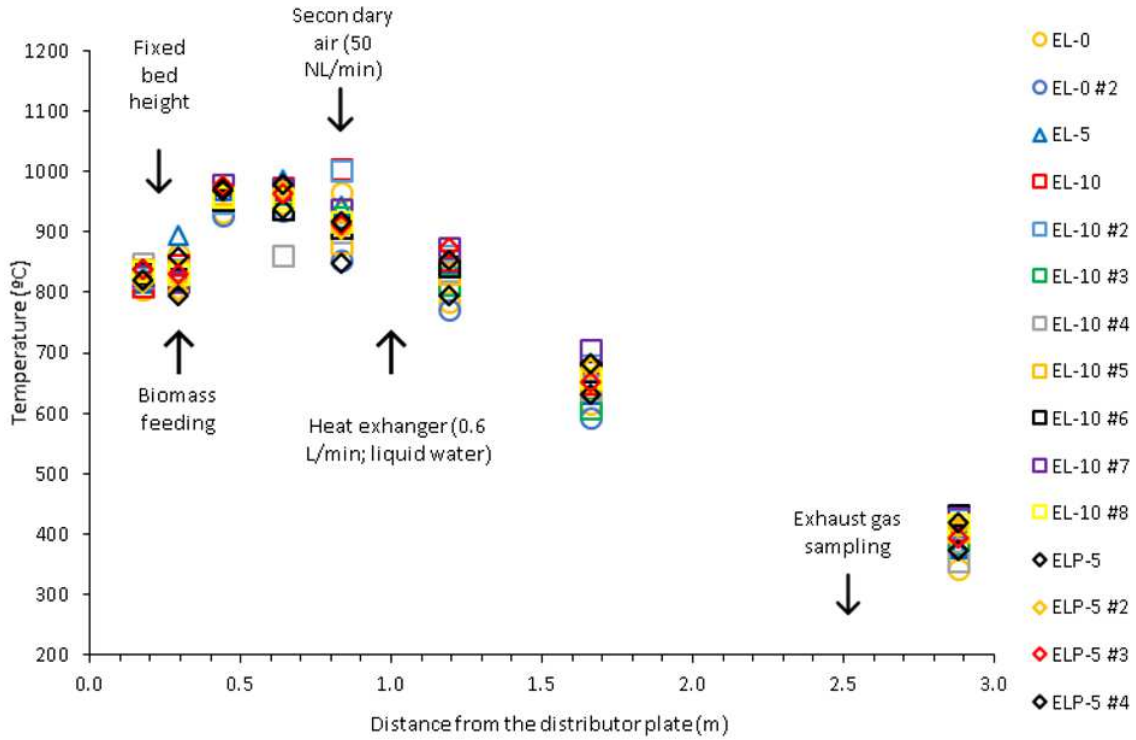
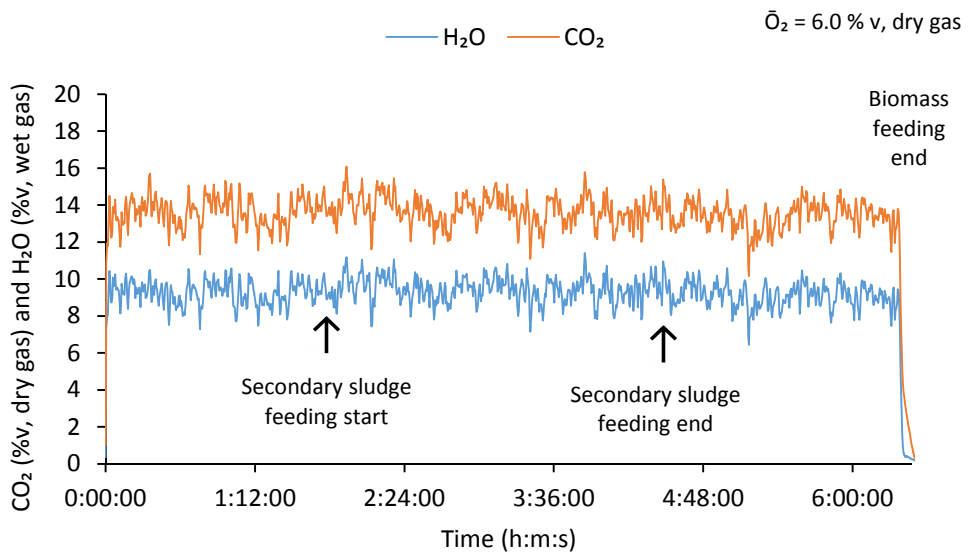
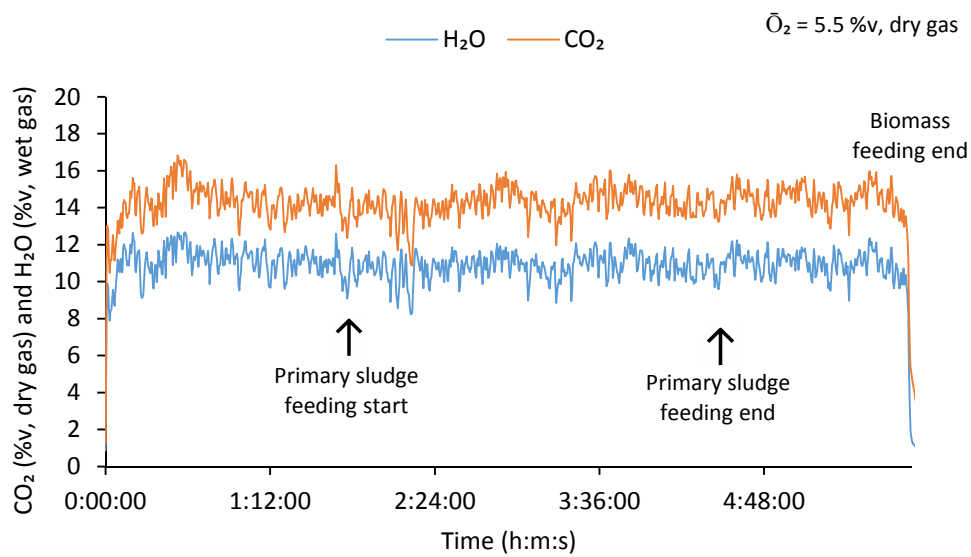


Figure 4 – Typical CO_2 and H_2O concentration along time in the exhaust gases for (a) EL-10 #7 and (b) ELP-5 #3. Experiment reference according to Table 3.

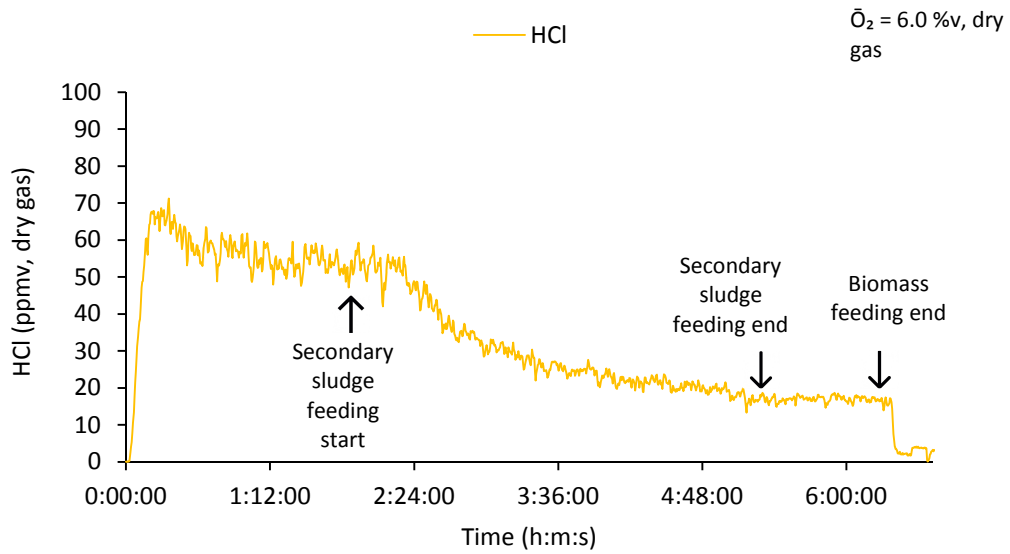


(a)

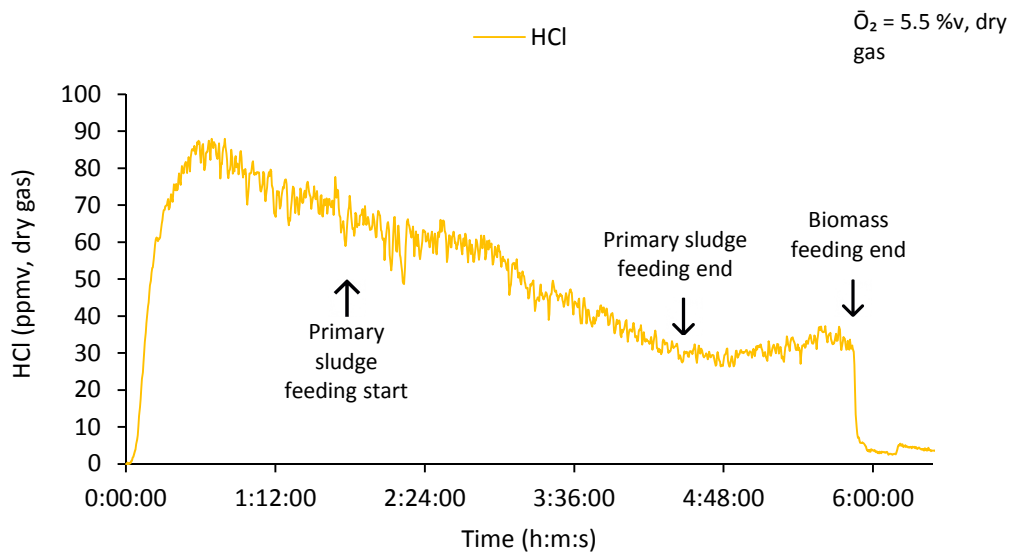


(b)

Figure 5 – Typical HCl concentration along time in the exhaust gases for (a) EL-10 #7 and (b) ELP-5 #3. Experiments reference according to Table 3.



(a)



(b)

Figure 6 – HCl concentration along time (30 minutes moving average) for the different combustion experiments performed. Experiments reference according to Table 3.

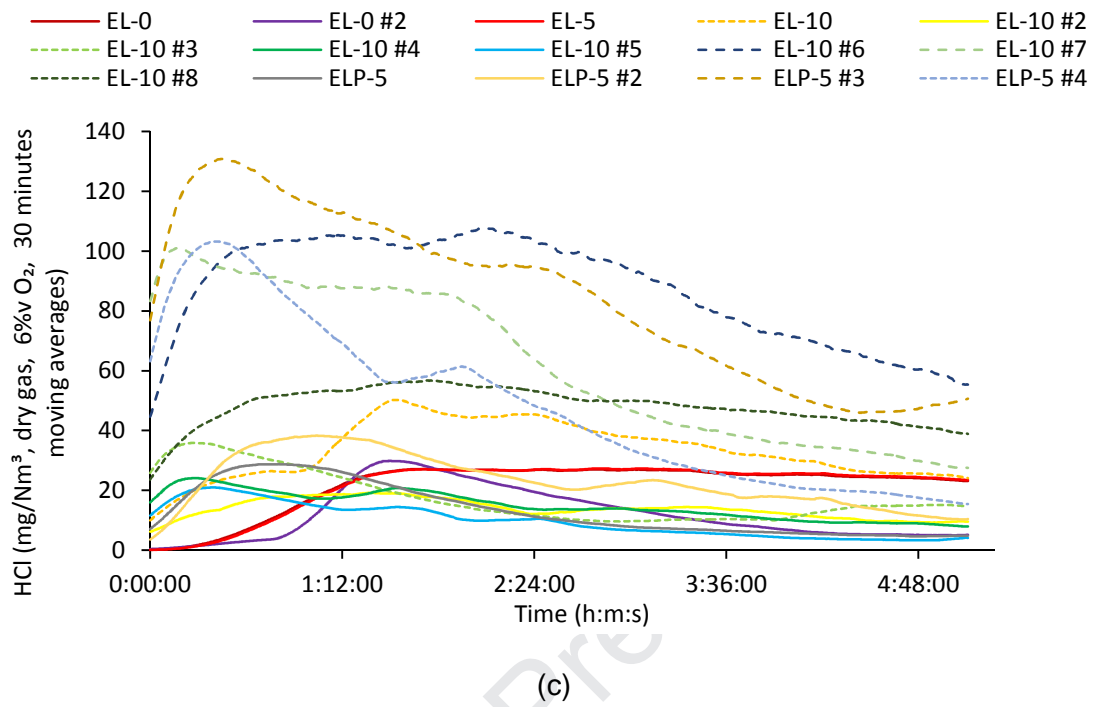
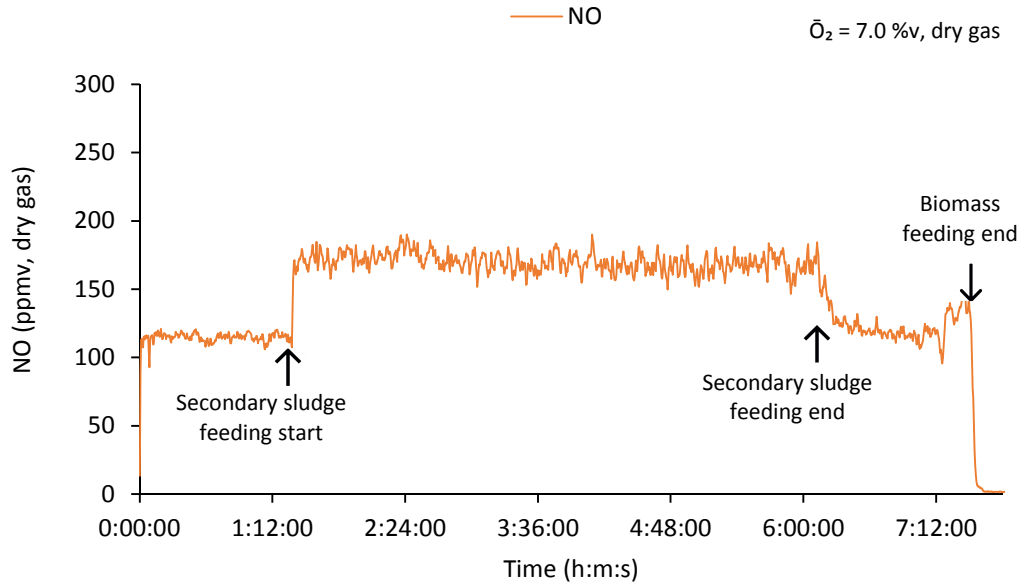
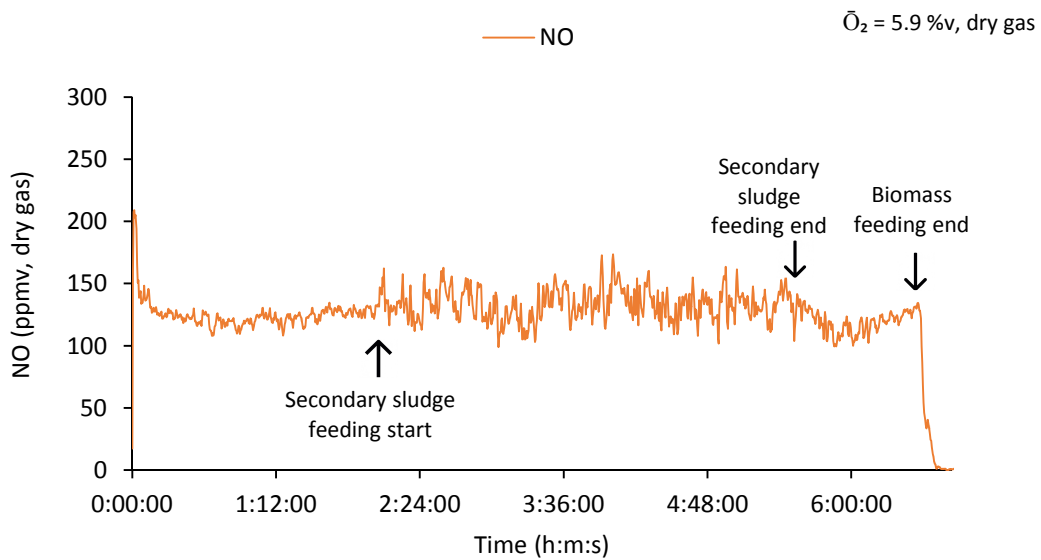


Figure 7 – Typical NO concentration along time in the exhaust gases for (a) EL-10, (b) EL-10#6, (c) EL-10 #7 and (d) ELP-5 #3. Experiments reference according to Table 3.

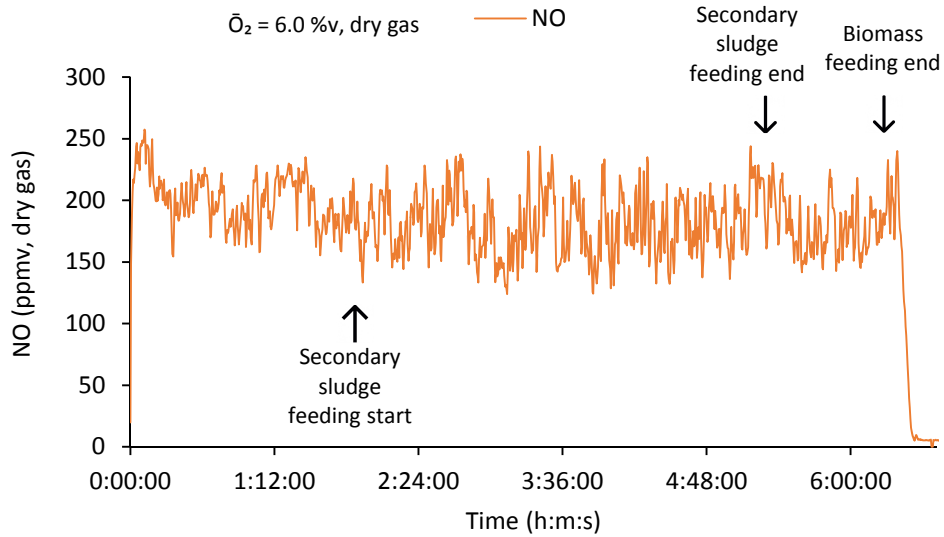


(a)

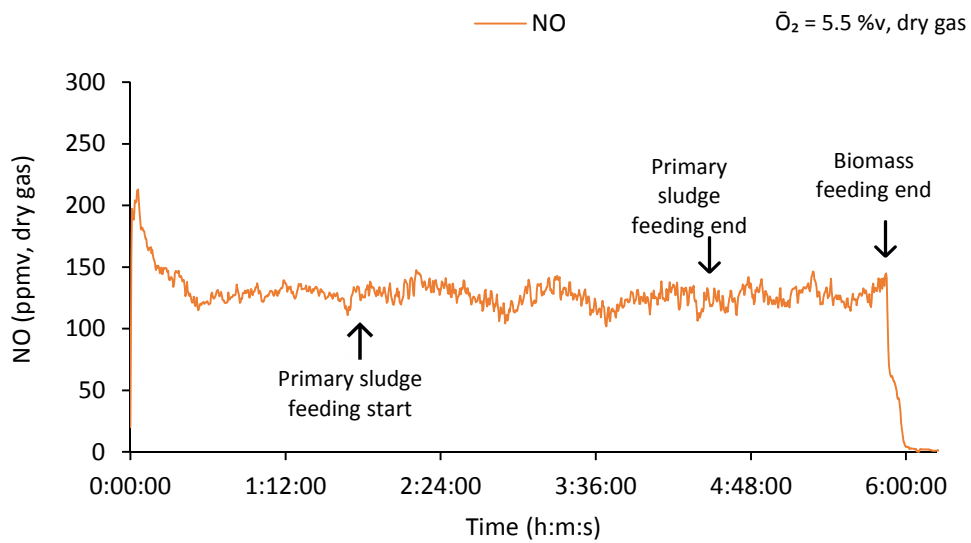


(b)

Figure 7 (continuation) – Typical NO concentration along time in the exhaust gases for (a) EL-10, (b) EL-10#6, (c) EL-10 #7 and (d) ELP-5 #3. Experiments reference according to Table 3.

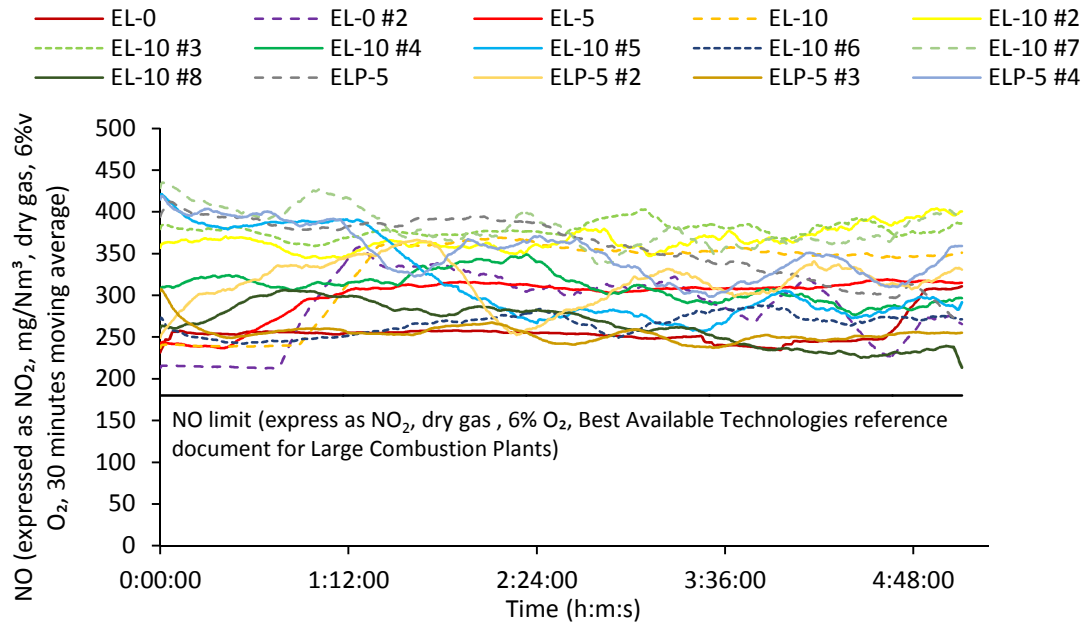


(c)



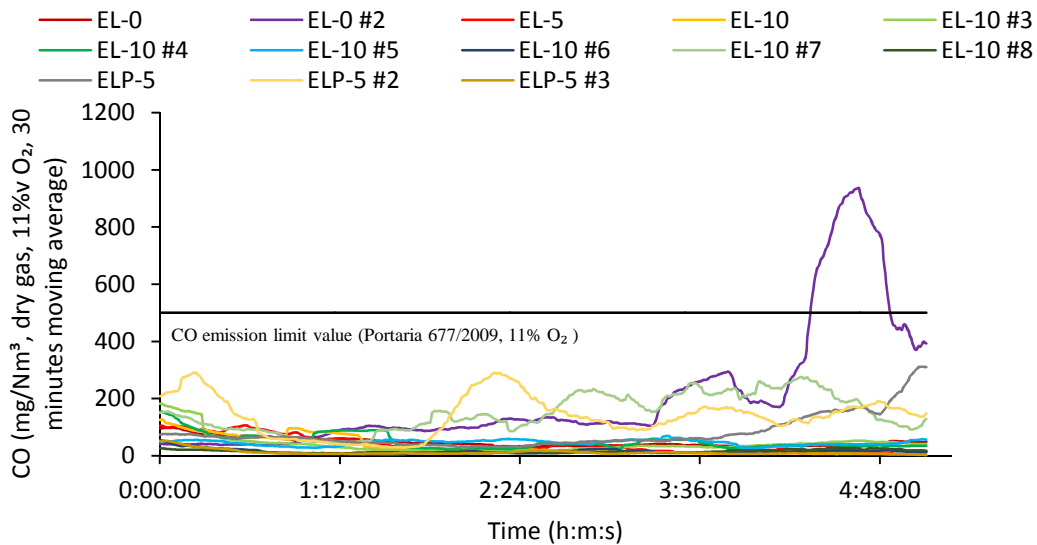
(d)

Figure 8 – NO concentration along time (30 minutes moving average) for the different combustion experiments performed and comparison with the limit value referred on the BAT reference document for Large Combustion Plants (IPPC 2016, 2016). Experiments reference according to Table 3.

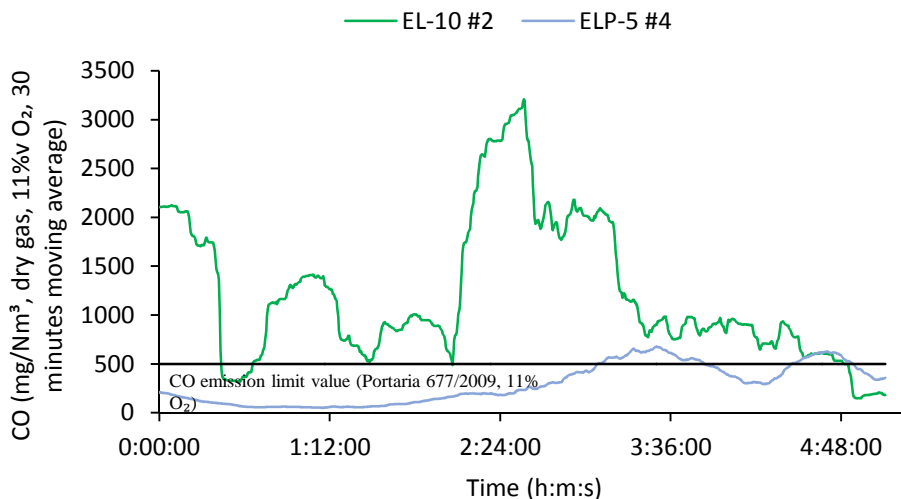


(e)

Figure 9 - CO concentration along time (30 minutes moving average) for the different combustion experiments performed and comparison with the limit value referred to biomass boilers in the Portuguese legislation, in Portaria 677/2009 (Governo de Portugal, 2009): (a) experiments with lower CO concentration values and (b) experiments with higher CO concentration values. Experiments reference according to Table 3.



(a)



(b)

Figure 10 - SO₂ concentration along time (30 minutes moving average) for the different combustion experiments performed and comparison with the limit value referred to biomass boilers in the Portuguese legislation, in Portaria 677/2009 (Governo de Portugal, 2009). Experiments reference according to Table 3.

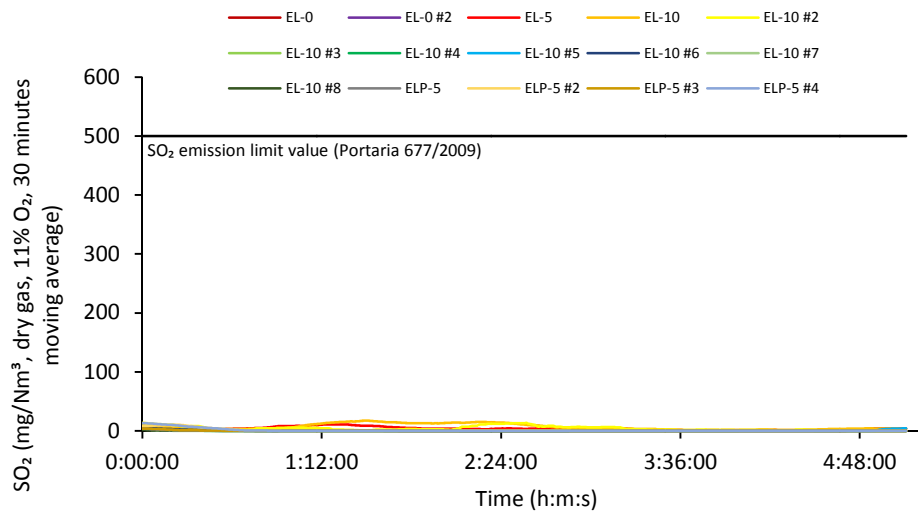
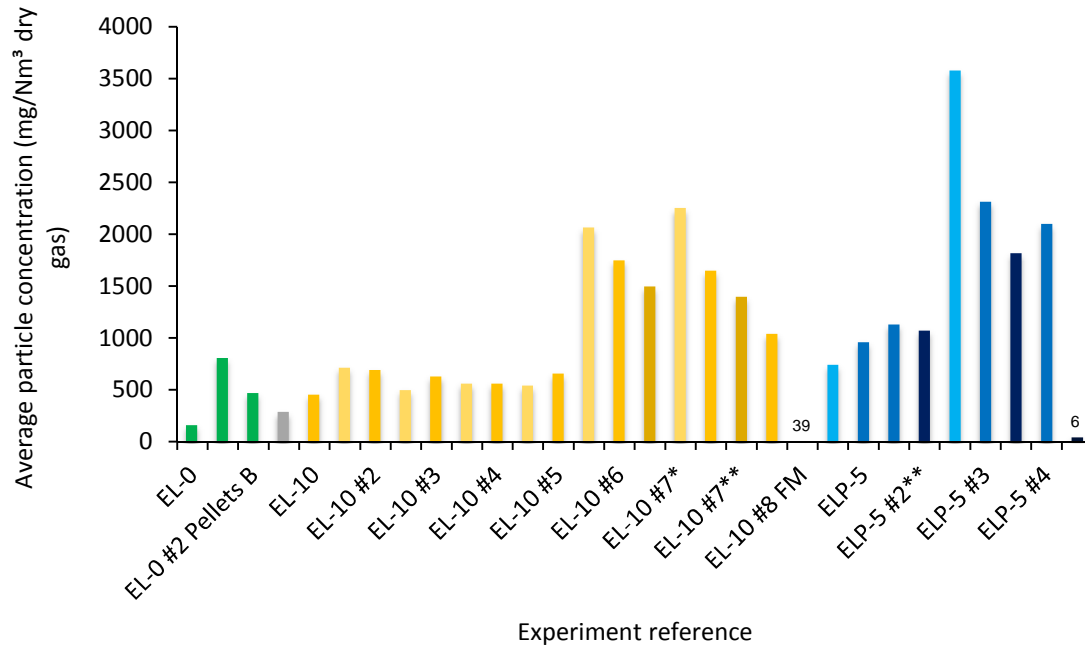


Figure 11 – Average particle (fly ash) concentration in the exhaust gases during the combustion experiments. The gas sampling was performed after the cyclone, except for references with FM, where the gas sampling was downstream of the bag filter. Experiments reference according to Table 3.

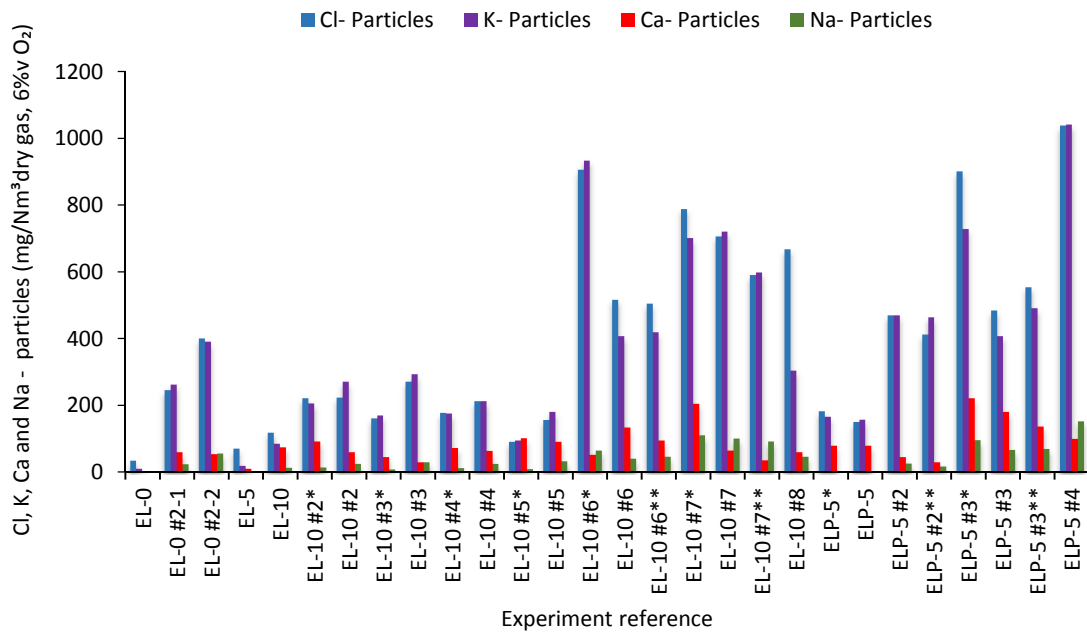


*- Only RFB, before introducing sludge;

**- Only RFB, after the co-combustion process of sludge with RFB;

FM- gas sampling after the bag filter.

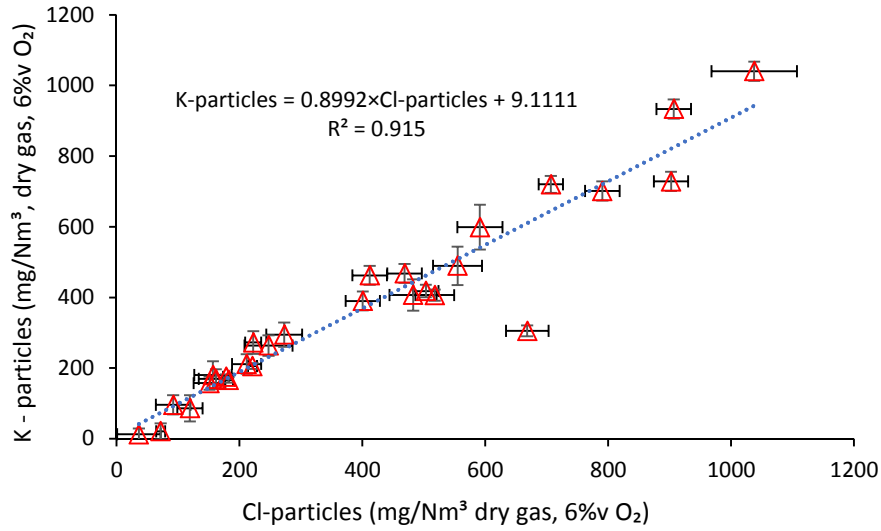
Figure 12 – Average Cl, K, Ca and Na concentration emitted associated with the fly ashes present in the exhaust gases during the combustion experiments. These elements were measured as ion Cl^- , K^+ , Ca^{2+} and Na^+ , and expressed as mg chemical element/ Nm^3 dry gas, corrected to 6%v O_2 . Sampling was performed downstream the cyclone (Figure 1). Experiments reference according to Table 3.



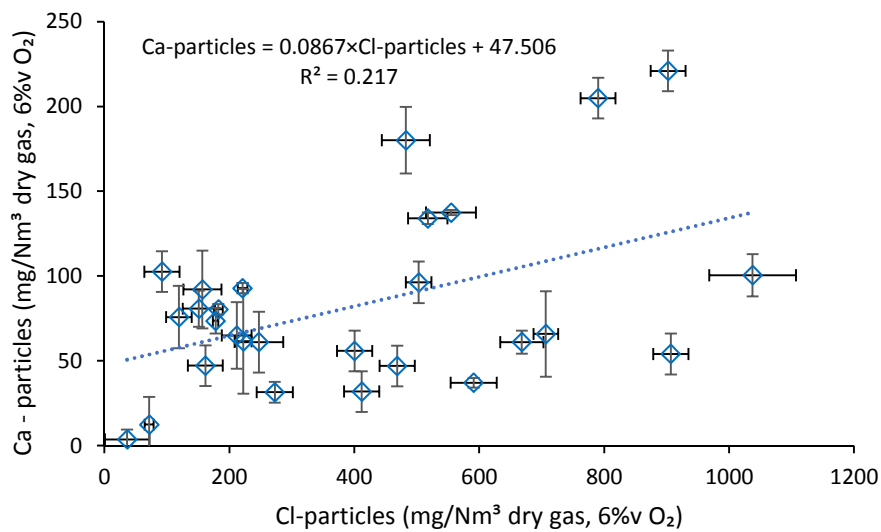
*- Only RFB, before introducing sludges;

** - Only RFB, after the co-combustion process of sludges with RFB.

Figure 13 – Relation between the content of K, Ca and Na with Cl in the fly ashes present in the exhaust gases during the combustion experiments: (a) K and Cl, (b) Ca and Cl and (c) Na and Cl.

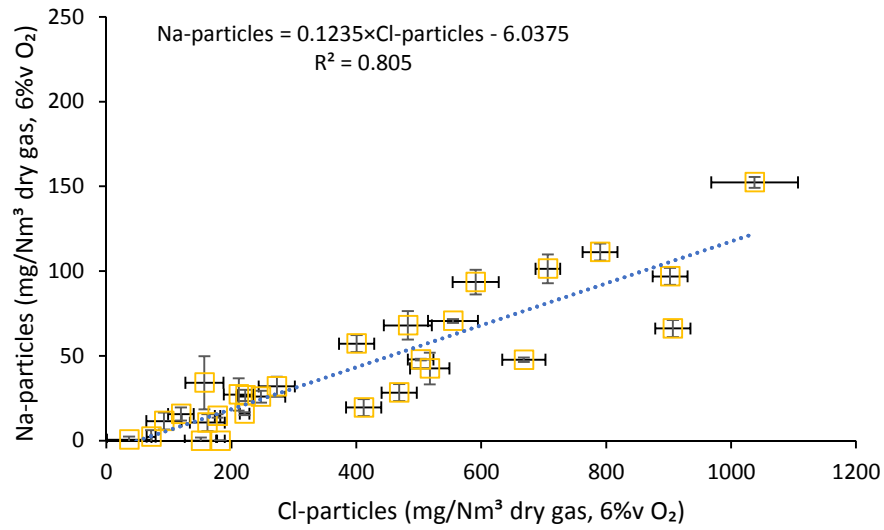


(a)



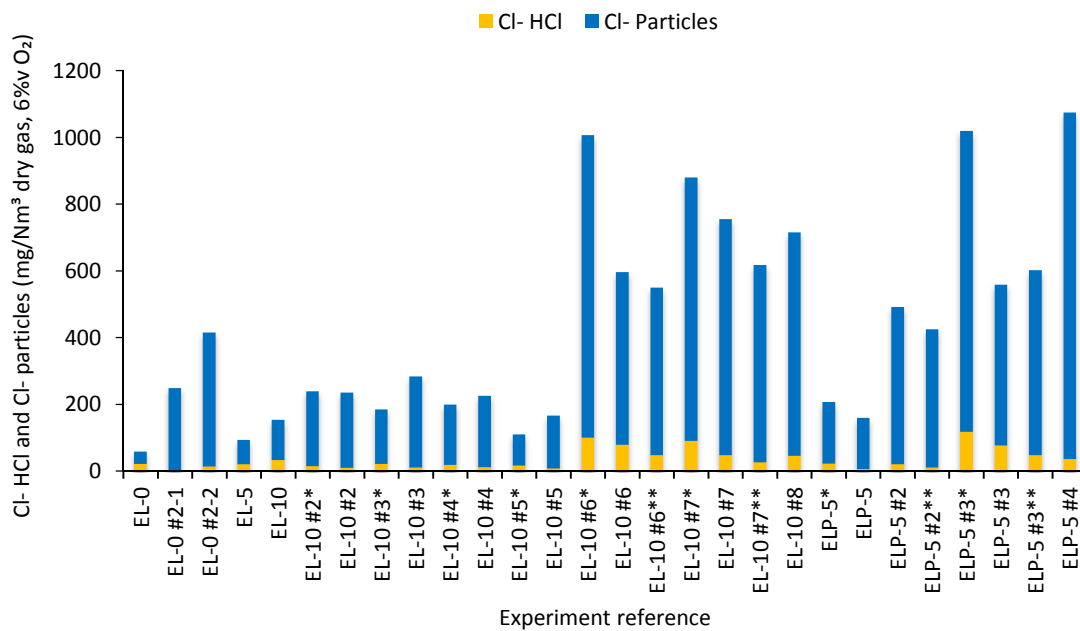
(b)

Figure 13 (continuation) – Relation between the content of K, Ca and Na with Cl in the fly ashes present in the exhaust gas during the combustion experiments: (a) K and Cl, (b) Ca and Cl and (c) Na and Cl.



(c)

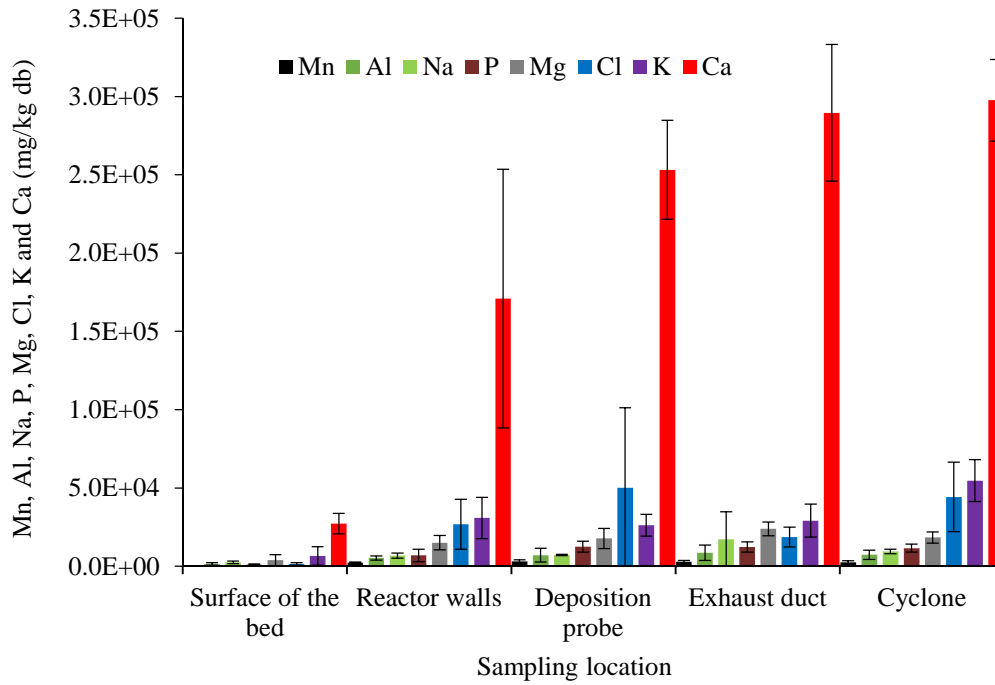
Figure 14 – Average Cl concentration in the solid phase, measured as ion Cl^- in fly ashes (denoted as Cl-particles), and expressed as $\text{mg Cl}/\text{Nm}^3$ dry gas corrected to 6%v O_2 , and in gaseous phase (denoted as Cl-HCl), measured as HCl in the flue gas and expressed as $\text{mg Cl}/\text{Nm}^3$ dry gas corrected to 6%v O_2 , in the exhaust gases during the combustion experiments. Sampling was performed downstream of the cyclone (Figure 1). Experiments reference according to Table 3.



*- Only RFB, before introducing sludges;

**- Only RFB, after the co-combustion process of sludges with RFB.

Figure 15 – Average composition (Ca, K, Mg, P, Na, Al, Mn and Cl) (and respective standard deviation) of the ashes deposited or settled in different locations of the combustion system.



Highlights

1. Co-combustion of residual forest biomass and sludge is shown as a valid valorization option;
2. Process stability was attained and demonstrated;
3. NO, CO and HCl emissions did not increase with sludge addition.

Journal Pre-proof

Declaration of interests

The authors declare that they have no known competing financial interests or personal relationships that could have appeared to influence the work reported in this paper.

The authors declare the following financial interests/personal relationships which may be considered as potential competing interests:

Daniel Louro Pereira *Luís Tarelho* *Teresa Vieira Nunes*
Miguel Baptista
Manuel António Almeida de Sá